AD-A039 010 AERONAUTICAL RESEARCH ASSOCIATES OF PRINCETON INC N J F/G 20/5
MODELING OF TURBULENT MIXING AND REACTIONS IN CHEMICAL LASERS.(U)
JAN 77 A K VARMA, E S FISHBURNE, R A BEDDINI F44620-75-C-0026
UNCLASSIFIED AFOSR-TR-77-0584 NL

1 OF 1
AD A039010

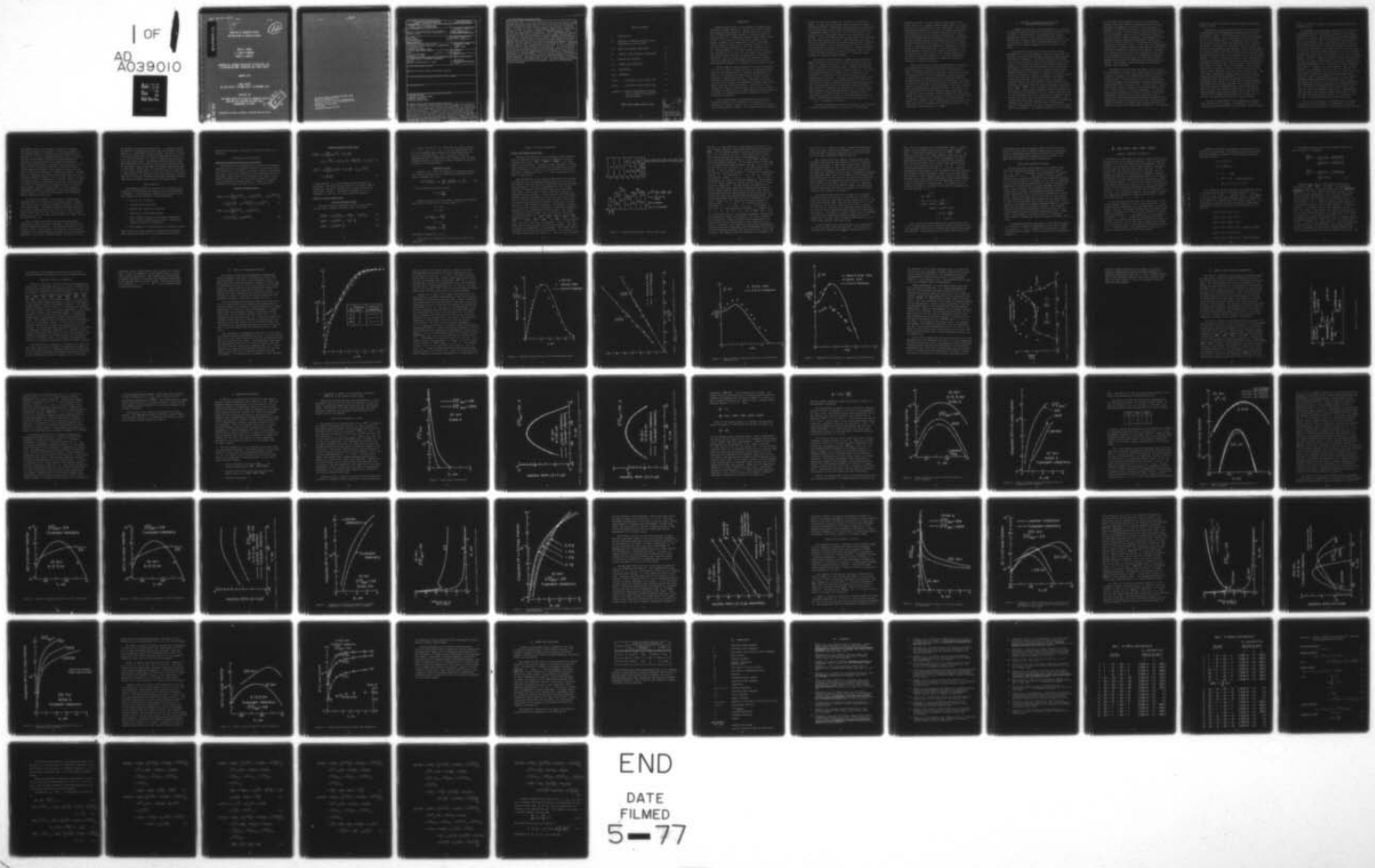

END

DATE FILMED
5-77

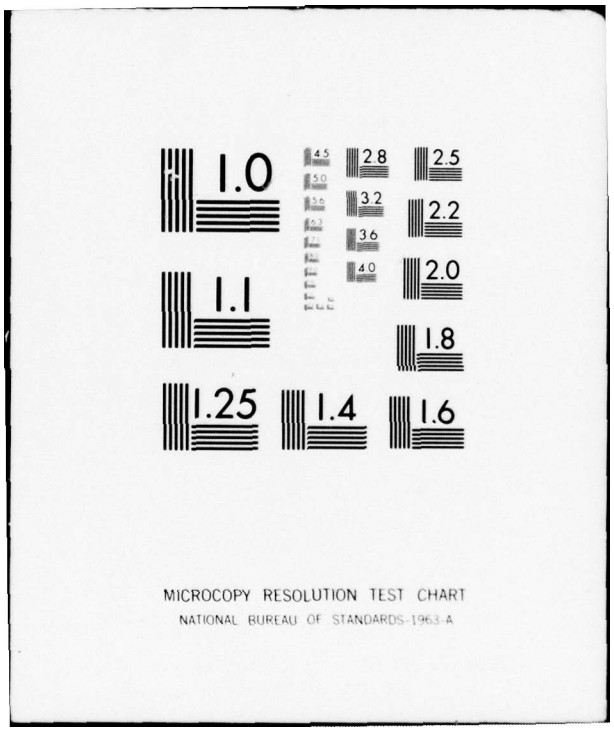
1.0
1.1
1.25
1.4
1.6
1.8
2.0
2.2
2.5
2.8
3.2
3.6
4.0
4.5
5.0
5.6
6.3
7.1
8.0
9.0
10.0
MICROCOPY RESOLUTION TEST CHART
NATIONAL BUREAU OF STANDARDS-1963-A

(12)

MODELING OF TURBULENT MIXING AND REACTIONS IN CHEMICAL LASERS

ASHOK K. VARMA
E. STOKES FISHBURNE
ROBERT A. BEDDINI

AERONAUTICAL RESEARCH ASSOCIATES OF PRINCETON, INC.
50 WASHINGTON ROAD, PRINCETON, NEW JERSEY 08540

JANUARY 1977

FINAL REPORT
FOR THE PERIOD 1 OCTOBER 1974 - 30 NOVEMBER 1976

PREPARED FOR

AIR FORCE OFFICE OF SCIENTIFIC RESEARCH (AFSC)
BUILDING 410, BOLLING AIR FORCE BASE
WASHINGTON, DC 20332

APPROVED FOR PUBLIC RELEASE; DISTRIBUTION UNLIMITED

SECURITY CLASSIFICATION OF THIS PAGE *(When Data Entered)*

REPORT DOCUMENTATION PAGE

READ INSTRUCTIONS BEFORE COMPLETING FORM

1. REPORT NUMBER: AFOSR - TR-77-0584	2. GOVT ACCESSION NO.
3. RECIPIENT'S CATALOG NUMBER	
4. TITLE *(and Subtitle)*: MODELING OF TURBULENT MIXING AND REACTIONS IN CHEMICAL LASERS,	5. TYPE OF REPORT & PERIOD COVERED: FINAL rept. 1 Oct 74-30 Nov 76,
	6. PERFORMING ORG. REPORT NUMBER
7. AUTHOR(s): ASHOK K. VARMA, E. STOKES FISHBURNE, ROBERT A. BEDDINI	8. CONTRACT OR GRANT NUMBER(s): F44620-75-C-0026 new
9. PERFORMING ORGANIZATION NAME AND ADDRESS: AERONAUTICAL RESEARCH ASSOCIATES OF PRINCETON INC, 50 WASHINGTON ROAD, PRINCETON, NEW JERSEY 08540	10. PROGRAM ELEMENT, PROJECT, TASK AREA & WORK UNIT NUMBERS: AO 3170/1, 62301E - TE20
11. CONTROLLING OFFICE NAME AND ADDRESS: DARPA, 1400 WILSON BOULEVARD, ARLINGTON, VA 22209	12. REPORT DATE: Jan 77
	13. NUMBER OF PAGES: 82 (85p.)
14. MONITORING AGENCY NAME & ADDRESS *(if different from Controlling Office)*: AIR FORCE OFFICE OF SCIENTIFIC RESEARCH/NA, BLDG 410, BOLLING AIR FORCE BASE, D C 20332	15. SECURITY CLASS. *(of this report)*: UNCLASSIFIED
	15a. DECLASSIFICATION/DOWNGRADING SCHEDULE

16. DISTRIBUTION STATEMENT *(of this Report)*

Approved for public release; distribution unlimited.

17. DISTRIBUTION STATEMENT *(of the abstract entered in Block 20, if different from Report)*

18. SUPPLEMENTARY NOTES

19. KEY WORDS *(Continue on reverse side if necessary and identify by block number)*

TURBULENCE MODELING
TURBULENCE IN CHEMICAL LASERS
TURBULENT SHEAR FLOWS
TURBULENT REACTING FLOWS

20. ABSTRACT *(Continue on reverse side if necessary and identify by block number)*

A complete second-order closure program for the investigation of compressible, turbulent, reacting shear layers has been developed at ARAP. The equations for the means and the second-order correlations are derived from the time-averaged Navier-Stokes equations. The equations contain third- and higher- order correlations, which have to be modeled in terms of the lower-order correlations. The program uses fluid mechanical turbulence models developed ~~by us and other investigators~~ over the last two decades. The analysis of reacting flows introduces the need for modeling additional scalar correlations. ARAP has developed a

DD FORM 1 JAN 73 1473 EDITION OF 1 NOV 65 IS OBSOLETE

UNCLASSIFIED 008 400 mt

SECURITY CLASSIFICATION OF THIS PAGE (When Data Entered)

"typical eddy" model for the joint probability density function of all the scalars. The ARAP second-order closure model for turbulent reacting flows has been used to study the mixing and chemical reaction in the initial region of a DF chemical laser. A majority of current HF and DF chemical lasers operate at cavity pressures of the order of 10 torr. The flow Reynolds numbers in these devices are of the order of 10^3, and turbulent transport is unimportant except in a small initial region downstream of the nozzle exit. Future laser systems are expected to operate at higher cavity pressures and turbulent transport processes will be more important. The effects of various turbulence parameters on the mixing and reactions in the chemical laser are quite complex. The program has been used to parametrically study the effect of turbulence variables-intensity q^2, scale Λ, and the turbulence-chemistry interaction represented by the mixedness correlation $\overline{\alpha'\beta'}/\bar{\alpha}\bar{\beta}$. The flow conditions correspond to the AFWL MESA IV nozzle. A simplified reaction scheme is used to study the production of DF(v), v= 1-4. Calculations have been made for cavity pressures of 10 and 100 torr. The results show that for 10 torr cavity pressure, there are very significant effects of the initial turbulence amplitude and turbulence scale on the formation of various DF vibrational levels. Different combinations of q^2 and Λ could lead to improvement or degradation in laser performance. At 100 torr operating pressure, the flowfield has a significant level of turbulence and the turbulence-chemistry interaction becomes important. Significant errors can result from the neglect of the mixedness correlations in the chemical source terms. The studies demonstrate the need for the use of a second-order closure approach to predict the nonequilibrium turbulent flowfields.

TABLE OF CONTENTS

AFOSR Contract Number F44620-75-C-0026

I. INTRODUCTION

Chemical lasers offer a unique means of obtaining high intensity, coherent radiation. Unlike other types of lasers which require large amounts of external power, the chemical laser obtains lasing action through the energy released in a chemical reaction. Conventional chemical lasers employ either H_2 and F_2 or D_2 and F_2 as the principal reactants in the system. Normally, the lasing action occurs in the mixing region between a stream of gas containing primarily H_2 or D_2 and another stream containing F_2 or F and a diluent, e.g., He. The performance of the laser depends on the ability of the configuration to mix and react the gases over a distance sufficiently large that optical energy may be efficiently extracted. Thus, the proper mixing and subsequent chemical reactions producing excited chemical species is one of the most important problems in the design of a good chemical laser.

Current chemical lasers operate at low cavity pressures, 5-10 torr, in order to reduce the rate of collisional deactivation of the excited species. At these low pressures, the mixing of the reactants is predominantly through molecular diffusion, a rather slow process. If the mixing could be achieved at a more rapid rate then, conceivably, the rate of excitation would increase considerably, providing higher laser output power and overall efficiency. In addition, if the mixing could occur at a faster rate, then it may be possible to operate the laser cavity at higher pressures thereby reducing the problem of bringing the gas up to atmospheric pressure (supersonic diffusion).

A more rapid mixing of the reactants may be achieved through turbulence in the flowfield. The possible role of turbulence in chemical lasers can best be understood by examining the structure of flames. In a laminar flame the reactions

between the fuel and oxidizer are confined to a very narrow region. In this case, the primary mode of mixing is through molecular diffusion. Employing molecular diffusion coefficients, the so-called flame velocity may be theoretically calculated to a reasonable degree of accuracy. As the flow velocity is increased and the flow becomes turbulent, two observations can be made. First, the flame velocity is much higher and, secondly, the flame zone becomes very wide. The widening of the flame zone is an indication that the dominant mass transfer is through turbulent mixing. In this situation, the width of the flame zone approaches the scale of the turbulence. Unlike the laminar flame velocity, the prediction of the turbulent flame velocity is very difficult because of the lack of a sufficient understanding of turbulent reacting flows.

The chemical laser presents a somewhat similar situation. Laminar mixing produces a very thin zone of lasing action between the streams of reactants. As the flowfield becomes turbulent, the lasing zone becomes wider. Conventional chemical lasers operate in the transition regime in which the flow cannot be characterized as fully laminar or fully turbulent. The prediction of turbulence in the transition regime requires sophisticated techniques. Turbulent mixing models which do not consider the history of the turbulence, such as the eddy viscosity approach and the turbulent kinetic energy approach, may lead to considerable errors in predicting laser performance. This situation is particularly important in flow situations in which turbulence is introduced through various boundary layer trip devices. In these situations it is important that a theoretical approach be capable of treating variable turbulent scales, intensities, and distributions of energy among the u, v, and w components of velocity.

Although turbulence may enhance the mixing of the reactants, it may have adverse effects on the rates of the individual

chemical reactions. In the turbulent flame example cited above, the use of a laminar chemistry model leads to considerable error in the prediction of the flame width. The laminar chemistry model means that the rate of a particular reaction is determined only by the average concentrations of the reacting species and the local average temperature. Although the local average species concentrations have been determined through turbulent mixing, the reactants may, in fact, not be mixed on a molecular level which is required for the species to react. This may be illustrated by considering the initial mixing of black and white paint. After a few swirls of the mixing paddle, we can define an average concentration of the two paints over a small region. But, clearly these two are not mixed on the molecular level. It is this unmixedness which is of primary importance in treating the effects of turbulence on chemical reactions.

Fully realizing the problems associated with the theoretical prediction of turbulent reacting flowfields, A.R.A.P. began developing a turbulence code which could provide the types of information which are required to determine the effects of turbulence on the rates of individual chemical reactions. In addition, it was important that the turbulence model be invariant since it may be employed in flow situations for which no turbulence measurements are available to calibrate the model. A.R.A.P.'s second-order closure technique is the only turbulence model which meets these necessary criteria. This report will briefly describe the A.R.A.P. Reacting Shear Layer (RSL) code. In addition, we will present numerous computations showing the effects of initial turbulence scale, intensity, and distribution of turbulent energy on the generation of excited chemical species in a chemical laser. Furthermore, we will indicate the error which can be introduced when the adverse effects of the turbulence, the unmixedness, is ignored.

II. ANALYSIS OF TURBULENT REACTING FLOWS - DESCRIPTION OF THE RSL CODE

A complete second-order closure program for the analysis of chemically reacting turbulent flowfields is being developed at A.R.A.P. The philosophy of our second-order closure approach and details of the technique have been previously described in a number of reports and publications (Refs. 1,2). For the sake of completeness a detailed description of the models and the computer program have been included in this report.

The theoretical analysis of turbulent flows is made difficult by the closure problem; namely, that the number of unknowns in an exact time-averaged formulation always exceeds the number of equations. The problem becomes more complex in the case of turbulent reacting flows because of the larger number of fluctuating quantities that are involved and the appearance of certain new and difficult scalar correlations. One commonly used approach for the solution of the closure problem requires the development of models for the extra unknown correlations to obtain a closed set of equations which can then be solved by a variety of methods. One simple modeling approach that has long been used in the study of turbulent flows is an eddy viscosity or first-order closure approach. Models are developed for second-order correlations, e.g., $\overline{u_i' u_j'}$, $\overline{u_i' T'}$, etc., in terms of the mean quantities of the flow. This approach completely ignores the dynamics of the turbulence and considers it to be a "local" quantity; that is, the turbulence at a point in the flow is completely determined by the local values of the mean flow variables. The procedure has been quite successful in a number of engineering problems, but it suffers from the need to determine the empirical constants for each class of flows from direct experimental measurements. It appears unlikely that an "invariant"

or "universal" eddy transport theory can be developed. Further, there are a number of turbulent flows of interest for which the dynamics (or history) of the turbulence is important in determining the nature of the turbulence at a point in the flow. In this respect, the first-order closure or eddy transport concept is not a sufficiently powerful tool with which to study the motion. Some examples are flow problems involving large-scale atmospheric motions, flow involving chemical reactions, and the developing regions of classically self-similar flows. In the past, most engineering calculations of reacting flows have been made by ignoring the interaction between the turbulence and chemistry. However, it is generally accepted that the interaction between turbulence and chemical reactions is of considerable importance in many practical flow problems, and first-order closure methods are not capable of handling such nonequilibrium flow regions. Second-order closure techniques are required to analyze these flowfields.

Considerable advances have been made in recent years in the development of second-order closure models for nonreacting turbulent flows which have demonstrated improved predictive capability compared to the eddy viscosity or first-order closure models. A.R.A.P. has been one of the leading groups in the development of multi-equation, complete second-order closure modeling of turbulent flows. The application of these higher-order closure procedures to turbulent reacting flows is a natural extension of current technology. In a second-order closure procedure one develops transport equations for second-order correlations and solves them along with the equations for the mean fluid dynamic variables subject to the appropriate initial and boundary conditions. These equations contain third-order and higher-order correlations which are modeled in terms of the lower-order correlations. The research

effort of a number of groups is directed toward establishing suitable models.

Considerable success has been achieved in the prediction of incompressible and compressible nonreacting flows using second-order closure. The formulation of the problem differs from group to group. Launder and Spalding (Ref. 3), Bradshaw (Ref. 4), and Saffman (Ref. 5) consider only equations for the turbulent kinetic energy and turbulence scale in addition to the mean flow equations. Donaldson, Varma, and others at A.R.A.P. have developed a multi-equation closure scheme (Refs. 6, 7, 8) which retains individual equations for all the important second-order correlations in the problem and provides much more detailed information about the turbulence field than the simpler schemes. A.R.A.P.'s approach has been to select the models in the simplest possible way consistent with tensor invariance and available experimental data. The model must remain invariant with respect to changes in the flow geometry. The invariant modeling is an important feature in that the objective is to obtain a model applicable to a wide class of fluid flows. Data from simple, extensively studied flows can then be used to obtain the general model parameters for use in more complex flowfields where experimental measurements are difficult. This model, with the use of the same set of model parameters, has demonstrated excellent agreement with experimental data for a wide class of flowfields, such as free shear layers (Ref. 6), flat plate boundary layers (Ref. 6), axisymmetric jets and wakes, the planetary boundary layer (Ref. 7), and the decay of turbulent vortices (Ref. 8). Finson (Ref. 9) has also used multi-equation models with good results.

The use of second-order closure modeling for reacting flows is still in its infancy. In addition to the normal difficulties associated with the second-order closure analyses

effort of a number of groups is directed toward establishing suitable models.

Considerable success has been achieved in the prediction of incompressible and compressible nonreacting flows using second-order closure. The formulation of the problem differs from group to group. Launder and Spalding (Ref. 3), Bradshaw (Ref. 4), and Saffman (Ref. 5) consider only equations for the turbulent kinetic energy and turbulence scale in addition to the mean flow equations. Donaldson, Varma, and others at A.R.A.P. have developed a multi-equation closure scheme (Refs. 6, 7, 8) which retains individual equations for all the important second-order correlations in the problem and provides much more detailed information about the turbulence field than the simpler schemes. A.R.A.P.'s approach has been to select the models in the simplest possible way consistent with tensor invariance and available experimental data. The model must remain invariant with respect to changes in the flow geometry. The invariant modeling is an important feature in that the objective is to obtain a model applicable to a wide class of fluid flows. Data from simple, extensively studied flows can then be used to obtain the general model parameters for use in more complex flowfields where experimental measurements are difficult. This model, with the use of the same set of model parameters, has demonstrated excellent agreement with experimental data for a wide class of flowfields, such as free shear layers (Ref. 6), flat plate boundary layers (Ref. 6), axisymmetric jets and wakes, the planetary boundary layer (Ref. 7), and the decay of turbulent vortices (Ref. 8). Finson (Ref. 9) has also used multi-equation models with good results.

The use of second-order closure modeling for reacting flows is still in its infancy. In addition to the normal difficulties associated with the second-order closure analyses

of turbulent flows, the presence of finite rate chemical reactions introduces the problem of the proper treatment of the combined effects of concentration and temperature fluctuations. At A.R.A.P., Donaldson and Hilst (Ref. 10) studied low heat release chemical reactions and demonstrated the importance of keeping track of the species correlations. Order of magnitude errors can be made in the prediction of the reaction rate in practical problems if classical chemical source expressions (based on mean quantities alone) are used and the species and temperature correlations ignored. Spalding (Ref. 11) formulated an "eddy break up" model valid for large turbulence Reynolds numbers and for very fast chemical reactions to model the effect of turbulence on chemical reactions. Chemical kinetic effects are ignored and the rate of the reaction is taken to be proportional to dissipation rate of the macroscale eddies. Recently, Spalding (Ref. 12) has proposed a LaGrangian approach to the modeling of turbulent combustion which attempts to predict the development of the probability density functions in the flow.

The major new problem in the analysis of compressible reacting flows is the modeling of the large number of higher-order correlations of scalar fluctuations arising in the chemical source terms. The general approach being used by many of the research groups active in the field is to model the probability density function (pdf) for the scalars. These include Rhodes et al. (Ref. 13), Bray and Moss (Ref. 14), Libby (Ref 15), and Borghi (Ref. 16).

Most of these approaches still make many simplifying assumptions to make the problem tractable. Bray and Libby use the fast chemistry assumption. The approach of Borghi is very similar to ours, but he replaces the joint pdf of species and temperature by a one-dimensional pdf which is a very restrictive assumption. The A.R.A.P. approach models the joint pdf of all

the scalars in turbulent reacting flows. A procedure has been developed for constructing the pdf using the available information in a second-order closure analysis. The model is called the "typical eddy" model and involves representing the pdf by a set of delta functions of variable strengths and positions in the scalar phase space. The strengths and positions of these delta functions at every point in the flow are determined from the predicted values of the means and second-order correlations at that point. Kewley (Ref. 17) has recently used our concept of the "typical eddy" model in a study of turbulence effects in a chemical laser. The details of the models and the RSL program code for the analysis of general multi-step exothermic chemical reactions in turbulent shear flows are discussed below.

Basic Equations

The general conservation equations for a turbulent, compressible, multi-component reacting flow system are presented in Appendix A. The following, commonly used assumptions have been adopted for the derivation of these equations:

1. The gas is a continuum.
2. No body forces are present.
3. Radiant heat transfer is neglected.
4. There are no overall mass sources.
5. Mass diffusion occurs by a concentration gradient only. Fick's diffusion law is valid. Thermal and pressure diffusion are neglected.
6. Each component of the gas mixture is thermally perfect.

These equations contain a number of third-order and higher-order correlations that have to be modeled in terms of the

means and second-order correlations to obtain a closed set of equations.

Second-Order Closure Models

Modeling of Pressure Fluctuation Correlations

The results for compressible flows presented in Reference 6 indicated the need for improved modeling of the pressure diffusion correlations. New models for various pressure correlations following a consistent procedure have been developed during the past year. The procedure for developing these models is presented in Reference 18. We are currently engaged in testing these new pressure diffusion models to improve our program predictions for high Mach number flows. The models are:

Pressure diffusion terms

$$\overline{p'u_i'} = P_1\bar{\rho}\Lambda^2 \frac{\partial \bar{u}_m}{\partial x_n}\left[\frac{1}{2}(\overline{u'^n u_i'})_{,m} - \frac{1}{4}\left\{\delta_m^n(\overline{u_i'u'^p})_{,p} + g_{mi}(\overline{u'^n u'^p})_{,p}\right\}\right.$$

$$\left. + \frac{1}{2}\left\{\delta_m^n\,\overline{u_i'u'^p}_{,p} - g_{mi}\,\overline{u'^n u'^p}_{,p}\right\}\right] + P_2\bar{\rho}\Lambda q(\overline{u_i'u'^p})_{,p} \qquad (1)$$

$$\overline{p'h'} = P_1\bar{\rho}\Lambda^2 \frac{\partial \bar{u}_m}{\partial x_n}\left[(\overline{h'u'^n})_{,m} - \frac{1}{3}\,\delta_m^n(\overline{h'u'^\ell})_{,\ell}\right.$$

$$\left. + \frac{1}{3}\,\delta_m^n\,\overline{h'u'^\ell}_{,\ell}\right] + P_2\bar{\rho}\Lambda q(\overline{h'u'^\ell})_{,\ell} \qquad (2)$$

Tendency-toward-isotropy terms

$$\overline{p'u'_{i,j}} = P_3\bar{\rho}\,\frac{\partial \bar{u}_m}{\partial x_n}\left[g_{mj}\overline{u'^n u'_i} - \frac{1}{3}\,\delta^n_m\,\overline{u'_i u'_j} - \frac{1}{3}\,g_{ij}\,\overline{u'^n u'_m} + \frac{1}{9}\,\delta^n_m\,g_{ij}q^2\right] - \frac{1}{2}\,\frac{\bar{\rho}q}{\Lambda}\left[\overline{u'_i u'_j} - \frac{1}{3}\,g_{ij}q^2\right] \quad (3)$$

$$\overline{p'h'_{,i}} = P_3\bar{\rho}\,\frac{\partial \bar{u}_m}{\partial x_n}\left[\frac{1}{3}\,\delta^n_m\,\overline{u'_i h'} - \frac{1}{2}\,\delta^n_i\,\overline{u'_m h'} - \frac{1}{2}\,g_{mi}\,\overline{u'^n h'}\right] - 0.8\,\frac{\bar{\rho}q}{\Lambda}\,\overline{u'_i h'} \quad (4)$$

In these models, Λ is the turbulent scale length to be determined. The major change compared to the models used in References 6 and 19 is the addition of terms involving the mean strain $\partial\bar{u}_m/\partial x_n$. Reference 19 suggests $P_2 = 0.1$. Constants P_1 and P_3 are still under investigation.

Models for Other Correlations

Velocity diffusion terms

Following previous successful A.R.A.P. studies (Refs. 6, 19), we adopt a gradient diffusion model, as follows:

$$\overline{u'_i u'_j u'_k} = -V_c\Lambda q\left[(\overline{u'_i u'_j})_{,k} + (\overline{u'_j u'_k})_{,i} + (\overline{u'_k u'_i})_{,j}\right] \quad (5)$$

$$\overline{u'_i u'_j \phi'} = -V_c\Lambda q\left[(\overline{u'_i \phi'})_{,j} + (\overline{u'_j \phi'})_{,i}\right] \quad (6)$$

$$\overline{u'_i \phi' \phi'} = -V_c\Lambda q\left[(\overline{\phi'\phi'})_{,i}\right] \quad (7)$$

In Eqs. (6) and (7), ϕ' represents any scalar variable (T' , h' , c'_α , ρ' , etc.). V_c was established equal to 0.1 by comparing model results with experimental data in free jets and shear layers. Due to the lack of detailed experimental data in compressible and reacting flows, the same diffusion constant is used as an initial estimate for velocity diffusion of all correlations.

Dissipation terms

Lewellen et al. (Ref. 20) suggest that isotropic dissipation is more suitable than the anisotropic dissipation model used by Donaldson (Ref. 19).

$$g^{mn}\,\overline{u'_{i,m}u'_{j,n}} = g_{ij}\,\frac{q^2}{3\lambda^2} + \frac{a}{\Lambda^2}\left(\overline{u'_i u'_j} - g_{ij}\,\frac{q^2}{3}\right) \tag{8}$$

λ is the turbulent microscale length

$$\lambda^2 = \frac{\Lambda^2}{a + \frac{bq\Lambda}{\nu}}$$

Detailed studies of the flat plate incompressible boundary layer (Ref. 21) have led to a slight change in a :

$$a = 3.25$$

$$b = 0.125$$

$$g^{mn}\,\overline{T'_{,m}T'_{,n}} = s\,\frac{\overline{T'T'}}{\lambda^2} \tag{9}$$

$$s = 1.8$$

$$g^{mn}\overline{u'_{i,m}T'_{,n}} = s_T\,\frac{\overline{u'_i T'}}{\lambda^2} \tag{10}$$

The present program uses $s_T = 1$.

The models for dissipation of other scalars are of the same form.

Models for Scalar Correlations

A.R.A.P.'s "Typical Eddy" Model

The major new difficulty in second-order closure computations of turbulent reacting flows is the modeling of scalar correlations, such as $\overline{k'\alpha'}$, $\overline{k'\alpha'\beta'}$, $\overline{\alpha'\alpha'\beta'}$, etc., that appear in the equations. Recently, we have developed a "typical eddy" model that is very promising for the modeling of all such scalar correlations. Details of the development of the model are given in References 22 and 23. A brief description of the model is given below.

The construction of the "typical eddy" model is an attempt to define the joint probability density function (pdf) for all the scalars, using the available information from a second-order closure analysis. The pdf is represented by a set of delta functions of variable strengths and positions in the scalar phase space. The location of some of the delta functions is decided on physical grounds. The positions of the other delta functions and the strengths of all the delta functions at every point in the flow are determined from the values of the means and second-order correlations obtained at that point from the solution of their transport equations. The degrees of freedom in the model are limited by the number of independent parameters available in the second-order closure analysis. Our complete second-order closure program for a three species flow system provides information for 13 independent first and second-order correlations — $\bar{\alpha}$, $\bar{\beta}$, $\overline{\alpha'\beta'}$, $\overline{\alpha'\gamma'}$, $\overline{\beta'\gamma'}$, $\overline{\alpha'\rho'}$, $\overline{\beta'\rho'}$, $\overline{\rho'\rho'}$, $\bar{h}$, $\overline{h'h'}$, $\overline{\alpha'h'}$, $\overline{\beta'h'}$, and $\overline{\rho'h'}$ — so the complete model can have no more than 13 parameters. Figure 1 shows the model that we have selected after extensive studies. The model has exactly 13 parameters to be determined. The typical eddy is considered to have the following structure. For a fraction ε_1 , the eddy contains only the species α . The cell has a sensible

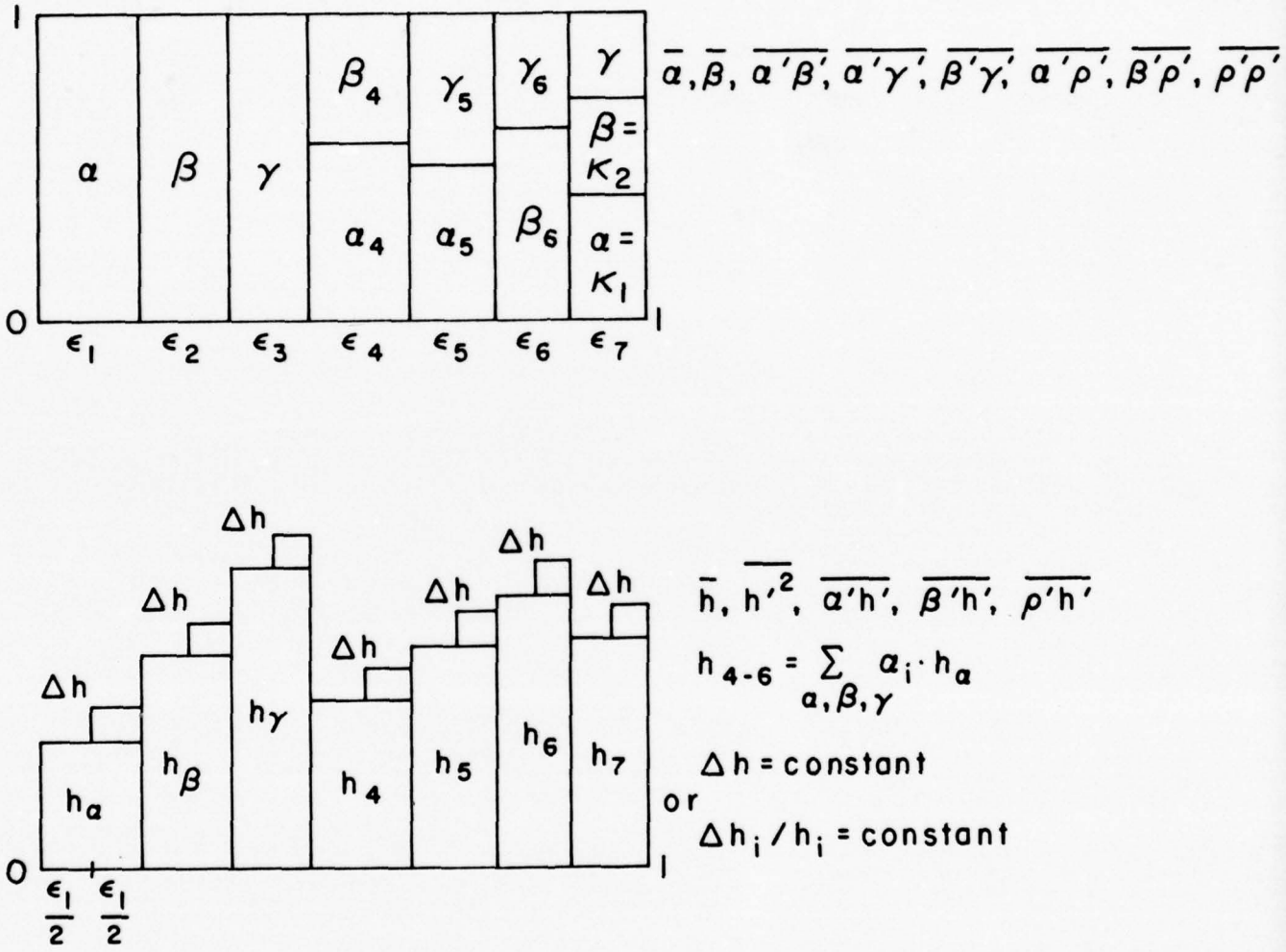

Figure 1. Complete three-species "typical eddy" model.

enthalpy h_α and, since for a single species flow from a constant enthalpy source the model must allow enthalpy fluctuations, $\overline{h'h'}$, due to boundary conditions and/or viscous heating, we add a Δh for half of the cell. For a single species flow, the enthalpy structure has just two parameters (h_α and Δh) to be calculated from the values of $\bar{h}$ and $\overline{h'h'}$ obtained from the transport equations. In the model currently being used in our reacting shear layer programs, the same Δh is used for all the cells. For a fraction ε_2, the eddy contains only species β with an enthalpy h_β, and for a fraction ε_3, the eddy has only the pure species γ and has the corresponding enthalpy h_γ. For fractions ε_4, ε_5, and ε_6, the eddy is assumed to contain α and β, α and γ, and β and γ, respectively, in a state of molecular mixedness. There appear to be two equally reasonable choices for the proportions of the species in these cells. One can consider the species to be present in either equal amounts or in amounts proportional to their average values at that point in the flow. The current program retains both of these options at the present time, and further test runs will indicate the more desirable model. Corresponding average values are used for the enthalpies of the cells. Finally, an ε_7 fraction of the eddy contains all three species α, β, and γ in a molecular mixture of proportions κ_1, κ_2, and $1 - \kappa_1 - \kappa_2$. The enthalpy of cell 7 is h_7. The model has 13 unknowns (ε_1 through ε_6, κ_1, κ_2, h_α, h_β, h_γ, h_7, and Δh) $\left(\text{note } \sum_{1-7} \varepsilon_i = 1\right)$ to be determined from the 13 available independent correlations by matching the moments of the model to the values predicted by the equations. Thus, the model can be constructed at any desired time from the second-order closure turbulence calculation in progress. Once the species and enthalpy distribution functions have been established, the corresponding distributions for the temperature, density, and the reaction rate can be constructed. The complete nonlinear Arrhenius rate expression can

be used for k ; there is no need to expand the exponential term. All scalar correlations required to close the system of second-order correlation equations can now be calculated from this joint probability density function.

The construction of the complete "typical eddy" model described above requires the solution of a set of nonlinear algebraic equations. A simplified "typical eddy" model was also proposed (Refs. 22, 23). This model does not consider the density fluctuation correlations in the construction of the model and, therefore, can only have 9 independent parameters. The simplified model results in a linear set of equations for the determination of the cell sizes in the species probability density function, and analytical closed form solutions have been obtained. In contrast, one has to resort to numerical solutions in the case of the complete model. The simplified "typical eddy" model was easier to implement for the initial testing of the concept of the model.

The simplification involves the neglect of the density correlations in the setting up of the model and, therefore, should be valid for flows where density changes are small. The simplified "typical eddy" model has been shown (Ref. 1) to be satisfactory for low heat release reacting flows. However, just how far one could use this simplified scheme could only be tested by actual computations and comparison to experimental measurements. Our studies on chemical laser flows and hydrogen-air flames where significant density changes are involved suggest that the more complete "typical eddy" model has to be used, as was expected, for these flows.

An even simpler model has been used in the calculations for the DF chemical laser reported here. In this model all third-order and higher-order <u>scalar</u> correlations are set to

zero. This is designated as the "secondary" model, as distinguished from the primary model which is the "typical eddy" model. Second-order correlations such as $\overline{T'\alpha'}$, $\overline{k'\alpha'}$, and others for which we do not carry transport equations, are now obtained up to second-order accuracy by expansion of explicit thermodynamic relations between the instantaneous variables. When the "typical eddy" model is used, these conversion relations are not necessary as the pdf for ρ,T and k can be constructed directly from the pdf of α_i and h using the thermodynamic relationships. The "secondary" model was initially used during the model development stage but some recent calculations (Ref. 1) have indicated that, at least for some simple reacting flows, the two models may predict quite similar results. It can be shown quite easily that the "secondary" model is not correct in a number of limiting cases. For example, in the reaction end limit for a system of three species undergoing the one step reaction $\alpha + \beta \rightarrow \gamma$,

$$\alpha\beta = 0$$

$$\bar{\alpha}\bar{\beta} + \overline{\alpha'\beta'} = 0$$

$$\bar{\alpha}\beta' + \alpha'\bar{\beta} + \alpha'\beta' - \overline{\alpha'\beta'} = 0$$

$$\bar{\alpha}\,\overline{\alpha'\beta'} + \overline{\alpha'\alpha'}\,\bar{\beta} + \overline{\alpha'\alpha'\beta'} = 0$$

$$\overline{\alpha'\alpha'\beta'} = -\bar{\alpha}\,\overline{\alpha'\beta'} - \bar{\beta}\,\overline{\alpha'\alpha'}$$

$$= \bar{\beta}\,\bar{\alpha}^2\left(1 - \frac{\overline{\alpha'\alpha'}}{\bar{\alpha}^2}\right)$$

$$\neq 0 \quad \text{in general}$$

Thus, setting the third-order scalar correlations to zero is not a proper model and the agreement between the results from the "secondary" model and the "typical eddy" model must be simply coincidental. The computations for the DF chemical laser will

be repeated later with the "typical eddy" model and the comparison of the two sets of results should be quite interesting. It is an interesting question why the results for some flows that have been studied are insensitive to the choice of the model for the higher-order scalar correlations.

Multi-Step Chemistry Procedure

The reacting shear layer program and the "typical eddy" model were originally developed for use with three species (α , β , and γ) flowfields, and only permitted the single-step reaction $\alpha + \beta \rightarrow \gamma$. The concept of such an overall reaction may be entirely sufficient in some combustion problems, but for most problems it is necessary to use a set of elementary reaction steps involving many species to correctly describe the system and to obtain results in better agreement with experiments. This conclusion is particularly valid with respect to trace species. Further, the elementary reactions have been studied extensively and the reaction rate parameters are better known. Ideally, one would like to keep track of each species and the correlation between each species and the other species as well as the correlation with certain flow properties. Unfortunately, this desire introduces an enormous number of equations which must be solved in an implicit fashion. The resulting computer time would be prohibitive to the point that the code would simply not be used for engineering calculations. Therefore, it was decided to construct a system for handling a finite number of species and reactions within the present framework.

To understand the basic philosophy of our reaction scheme, it is useful to consider the expression for the rate of change of a species, α , due to chemistry in a situation in which turbulence may be present. It can be shown that the expression reduces to:

$$\frac{d\bar{\alpha}}{dt} = -\bar{k}\bar{\alpha}\bar{\beta} - [\bar{k}\overline{\alpha'\beta'} + \bar{\alpha}\overline{k'\beta'} + \bar{\beta}\overline{k'\alpha'} + \overline{k'\alpha'\beta'}]$$

Laminar Turbulent Contribution

In the absence of turbulence, the rate of change of the species is simply given by the laminar expression. When turbulence is present, all of the other terms must be considered. The computation of these terms, and the other necessary correlations, is the reason the computer time becomes excessive. In the laminar case, such correlations are not required. Thus, the extension of laminar flow situations to hundreds of chemical species and reactions is straightforward since it only requires the addition of another equation for the conservation of mass of each added species. In the turbulent case, the addition of a new species requires the addition of at least three equations for the correlations with the primary flow variables plus an equation for the correlation with each of the other species in the flow. From a practical viewpoint, and the desire to maintain reasonable computation times, it was decided to "track" only three species: α , β , and γ .

In any diffusive reacting flow, one usually has two initially separate streams of fuel (α) and oxidizer (β). These streams are now considered to be known mixtures of a number of chemical species. The streams mix and react following a large number of elementary reactions and form a mixture of product species designated as γ . We assume that (1) the composition of mixtures α and β is fixed for the entire flowfield. There are no internal reactions among the species in these two reactant mixtures. (2) All the product species that compose γ are molecularly mixed. There are internal reactions within the γ species mixture. The composition of the mixture γ varies at different points across the flowfield.

Consider the following two-reaction system as an illustration of the procedure. The complete set of reactions that have been used in our studies of the DF chemical laser are presented in Table 1.

$$D_2 + F \xrightarrow{k_1} DF + D$$

$$F_2 + D \xrightarrow{k_2} DF + F$$

α	D_2	known
β	$He + F + F_2$	known proportions
γ	$He + D_2 + F_2 + D + F + DF$	

The interaction between turbulence and chemistry only has to be taken into account for reactions between α and β, α and γ, and β and γ. Species within γ are assumed to be molecularly mixed and, therefore, species correlations do not have to be considered for the internal reactions. For convenience, we rewrite the reaction system as given below, tagging each chemical species with the mixture that it is a part of:

$$D_2(\alpha) + F(\beta) \rightarrow DF(\gamma) + D(\gamma)$$

$$D_2(\alpha) + F(\gamma) \rightarrow DF(\gamma) + D(\gamma)$$

$$D_2(\gamma) + F(\beta) \rightarrow DF(\gamma) + D(\gamma)$$

$$D_2(\gamma) + F(\gamma) \rightarrow DF(\gamma) + D(\gamma) \quad \text{internal reaction}$$

$$F_2(\beta) + D(\gamma) \rightarrow DF(\gamma) + F(\gamma)$$

$$F_2(\gamma) + D(\gamma) \rightarrow DF(\gamma) + F(\gamma) \quad \text{internal reaction}$$

The chemical source terms for the component species can now be written. For example,

$$\frac{d\overline{D_2}(\alpha)}{dt} = - k_1\left[\overline{D_2}(\alpha)\overline{F}(\beta) + \overline{D_2'(\alpha)F'(\beta)}\right] - k_1\left[\overline{D_2}(\alpha)\overline{F}(\gamma) + \overline{D_2'(\alpha)F'(\gamma)}\right]$$

$$\frac{d\overline{D_2}(\gamma)}{dt} = - k_1\left[\overline{D_2}(\gamma)\overline{F}(\beta) + \overline{D_2'(\gamma)F'(\beta)}\right] - k_1\left[\overline{D_2}(\gamma)\overline{F}(\gamma)\right] \quad , \text{ etc.}$$

Transport equations are solved for the second-order correlations $\overline{\alpha'\beta'}$, $\overline{\alpha'\gamma'}$, and $\overline{\beta'\gamma'}$. The additional important assumption is made that quantities like $\overline{D_2'(\alpha)F'(\beta)}$, $\overline{D_2'(\alpha)F'(\gamma)}$, etc. can be simply calculated from these correlations as being proportional to the local mean composition of the mixture. The validity of this assumption has to be examined further, but it should not lead to large errors. The rate at which α or β react to form the product species γ is governed by the rate of the fastest reaction. In the above example, β is being lost due to the consumption of both $F(\beta)$ and $F_2(\beta)$. The reaction that causes the greater loss of β is the controlling step. If at some point in the flow, the reactions of $F(\beta)$ lead to the larger loss of β , then to maintain the constant composition of the β species mixture, corresponding amounts of $F_2(\beta)$ and $He(\beta)$ now become part of the γ species. The composiiton of γ has to be calculated at each point across the flowfield. The procedure operates within the framework of three overall species mixtures, and all the models and equations developed earlier can be used. The

only addition to the program is the solution of the mean species conservation equations for all the elemental species.

Numerical Solution of Equations

The use of the models for various third- and higher-order correlations, as described earlier, in the set of equations for the means and second-order correlations results in a closed set of equations. Equations for the mean variables $\bar{\rho}$, $\bar{u}_i$, $\bar{h}$, $\bar{\alpha}$, and $\bar{\beta}$ and the second-order correlations $\overline{u_i'u_j'}$, $\overline{h'h'}$, $\overline{u_i'h'}$, $\overline{\alpha'\beta'}$,, $\overline{\alpha'\gamma'}$, $\overline{\beta'\gamma'}$, $\overline{u_i'\alpha'}$, $\overline{u_i'\beta'}$, $\overline{u_i'\rho'}$, $\overline{h'\alpha'}$, and $\overline{h'\beta'}$ are solved in the present program. The use of the basic shear layer assumptions leads to a set of 23 independent coupled parabolic partial differential equations. The computer program actually solves a total of 30 equations; the redundant equations provide a check on the mass conservation in the program and on the accuracy of the numerical scheme. The numerical integration of the equations is performed by a forward-time-centered-space, quasi-implicit, upwind, finite differencing scheme. The nonlinear terms are handled by quasi-linearization, that is, by evaluating a portion of these terms at the known position, leaving only a linear term containing one of the unknowns. The linearized finite-difference equations are solved by the general tridiagonal algorithm; but, instead of solving a single large matrix (which would be very time consuming), the equations are grouped into smaller matrices and the system is solved in 10 separate passes. The program is running satisfactorily on our Digital Scientific Corporation META-4 computer.

The program has the capability of handling both fixed and free shear layer flows for planar and axisymmetric geometries. The initial profiles can be provided using a card or tape input or the program can generate appropriate smooth initial profiles given the properties of the two streams. If the turbulence

properties at the initial station are not known, we typically input a "spot" of turbulence at the initial station to start the turbulent calculations. The program uses a fourth-order polynomial expression to calculate the temperature dependence of the specific heat of various species. The molecular transport properties μ , μ^* , k , and D are calculated using a power law expression.

III. MODEL AND PROGRAM VERIFICATION

The principal objective of developing a higher-order closure turbulence model than the first-order closure eddy-viscosity models is to obtain a more "universal" model; a model which can be used for analysis of data for a wide class of flowfields with the use of the same invariant set of model constants. Such a model can then be used with a greater degree of confidence for predictive calculations of flow problems for which experimental data are not available or are difficult to obtain. Second-order closure models have shown significant promise of being such a predictive tool.

The fluid mechanical turbulence models being used in the A.R.A.P. second-order closure program have already been extensively tested by comparison of program predictions to experimental data in a variety of basic flow geometries. Previous publications have discussed studies on flat plate boundary layers (Ref. 6), the planetary boundary layer (Ref. 7), and axisymmetric jets and wakes (Ref. 24). Model and program verification studies that are of interest in connection with the analysis of the planar mixing flow in DF chemical lasers are our analyses of a two-dimensional wake and a heated planar jet (Ref. 1) and the mixing of two different species in a shear layer.

The experimental measurements in the wake of a thin plate were made by Chevray and Kovasznay (Ref. 25). Detailed measurements of the mean axial velocity profile and the Reynolds stress were made using hot wire probes. The experimental measurements are designated as Test Case 14 in data collected at the 1972 NASA Free Turbulent Shear Flows Conference (Ref. 26). Figure 2 compares the theoretical RSL program predictions for the mean axial velocity profiles at three axial stations with the measurements. The computations are generally in good agreement

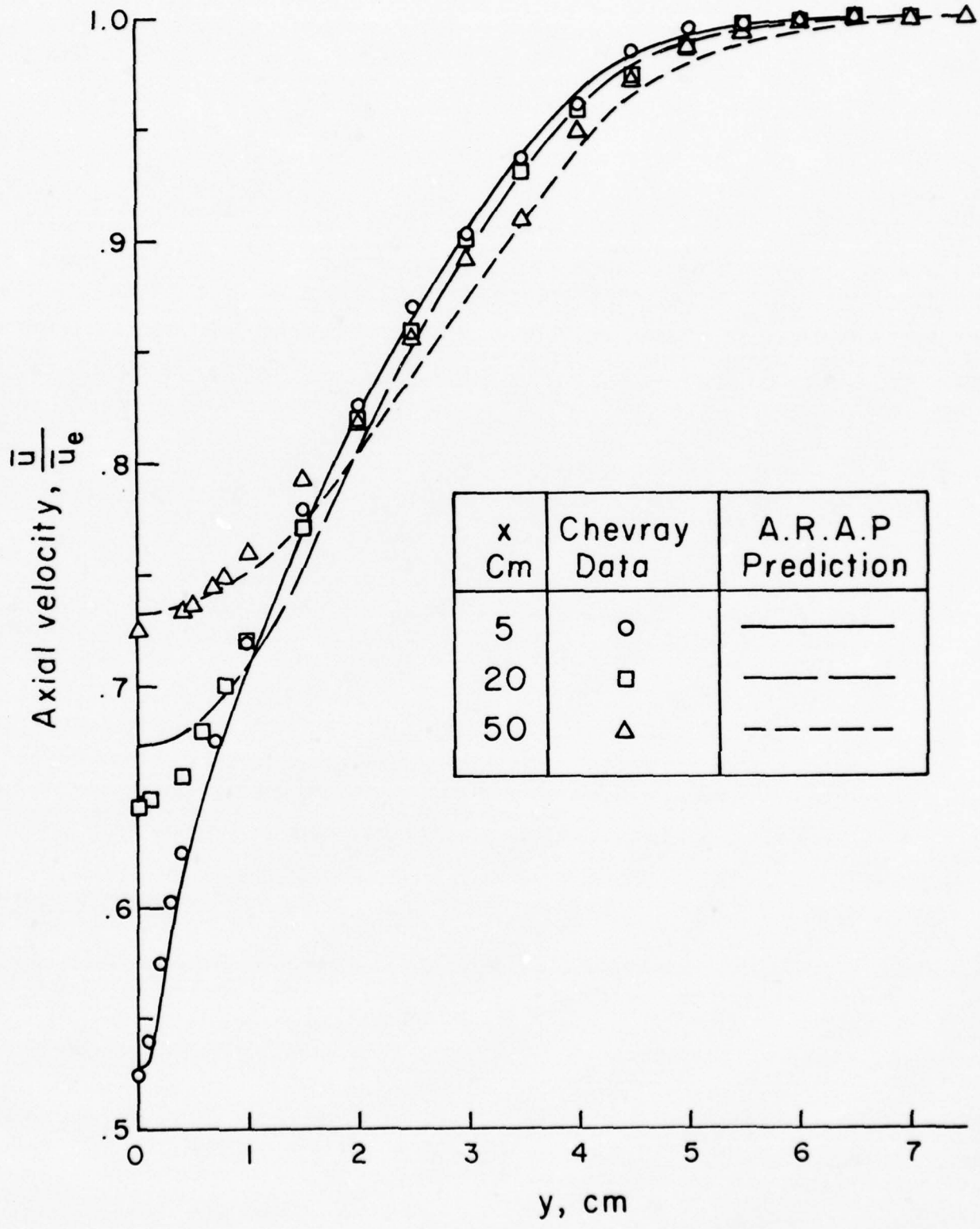

Figure 2. Mean axial velocity profiles in the two-dimensional wake.

with the data over the entire profile. There is some discrepancy between the predictions and the experiments as to the centerline velocity at $x = 20$ cm , the reason for which is not known at this time. Figure 3 shows the predicted profile for the Reynolds stress correlation $\overline{u'v'}$ at $x = 50$ cm . At this axial station, the computations are in good agreement with the data. Further downstream, at $x = 240$ cm , the peak value of the computed $\overline{u'v'}$ is about 25% lower than the experimental data, but the profile shape is in good agreement.

Davies, et al. (Ref. 27) and Uberoi and Singh (Ref. 28) have carried out extensive measurements of mean and turbulence quantities in heated plane turbulent jets. Figure 4 presents our program predictions for the decay of the mean velocity and temperature on the jet centerline and compares the predictions to the data of Ref. 27. The decay of the mean velocity is in excellent agreement with the data and the linear graph shows the self-preserving nature of the turbulent jet. At larger axial distances, the turbulence falls off and the decay rate deviates from the straight line. The decay of the centerline temperature is well-known to be faster than the velocity as shown here. The slope of the calculated temperature ($\theta = T - T_{ambient}$) decay rate is slightly smaller than Davies' experimental results. However, the overall agreement of the program predictions with experimental measurements is quite satisfactory. In the self-preserving region, the calculated values of $\overline{u'u'}^{1/2}/\bar{u}_{max}$ are 0.16 at the centerline and a peak value of 0.20 , in agreement with Davies' results of 0.18 and 0.21 , respectively, as shown in Figure 5. Figure 6 shows the results for the profile of $\overline{\theta'\theta'}^{1/2}/\bar{\theta}_{max}$ at $x/b = 20$. Our program predicts 0.22 at the center and a peak value of 0.31 at $y/\ell_\theta = 0.8$. Davies' measured values are significantly lower and the profile is virtually flat. Uberoi and Singh have also made temperature correlation measurements in a plane heated jet

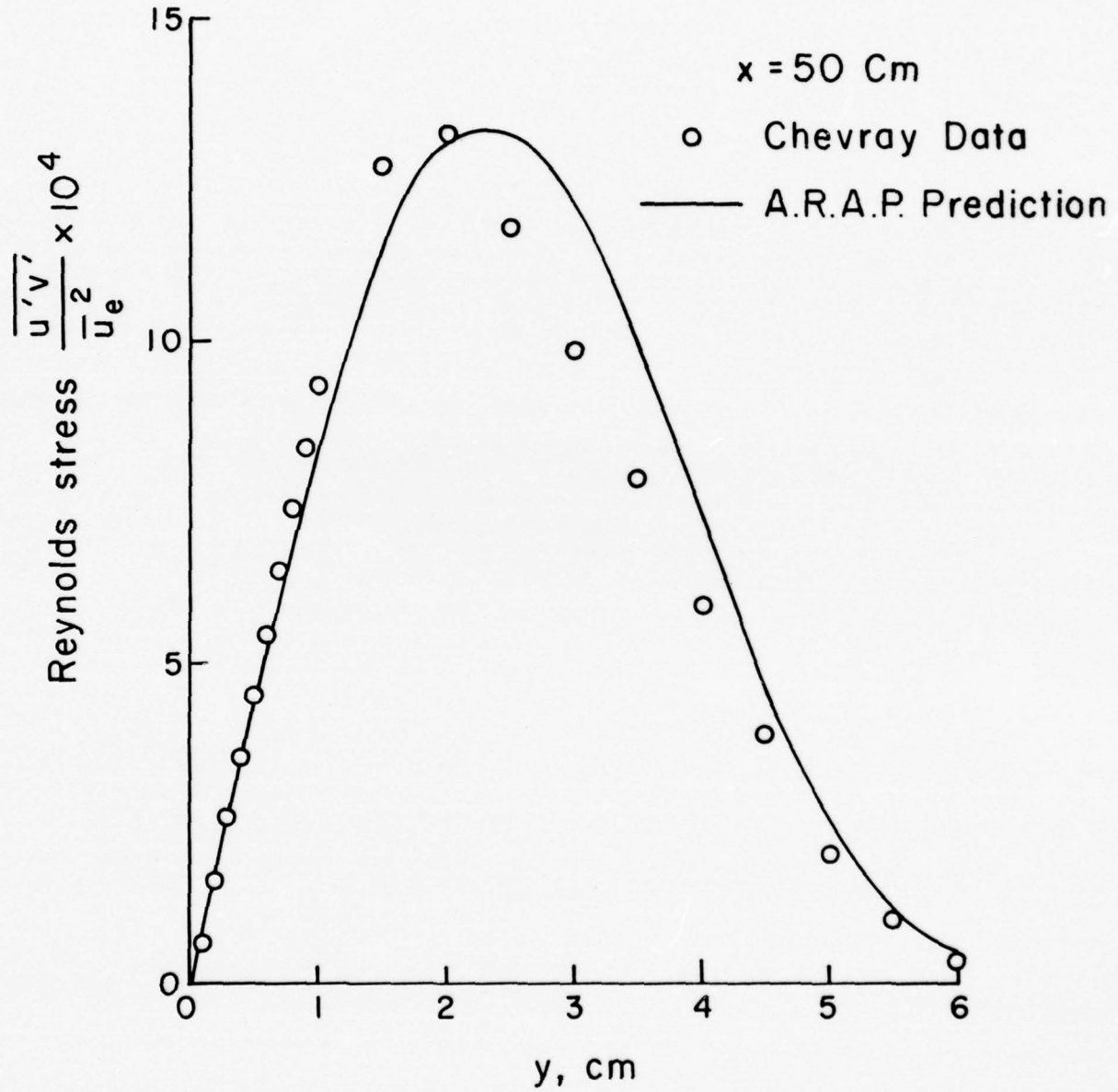

Figure 3. Reynolds stress profile in the two-dimensional wake.

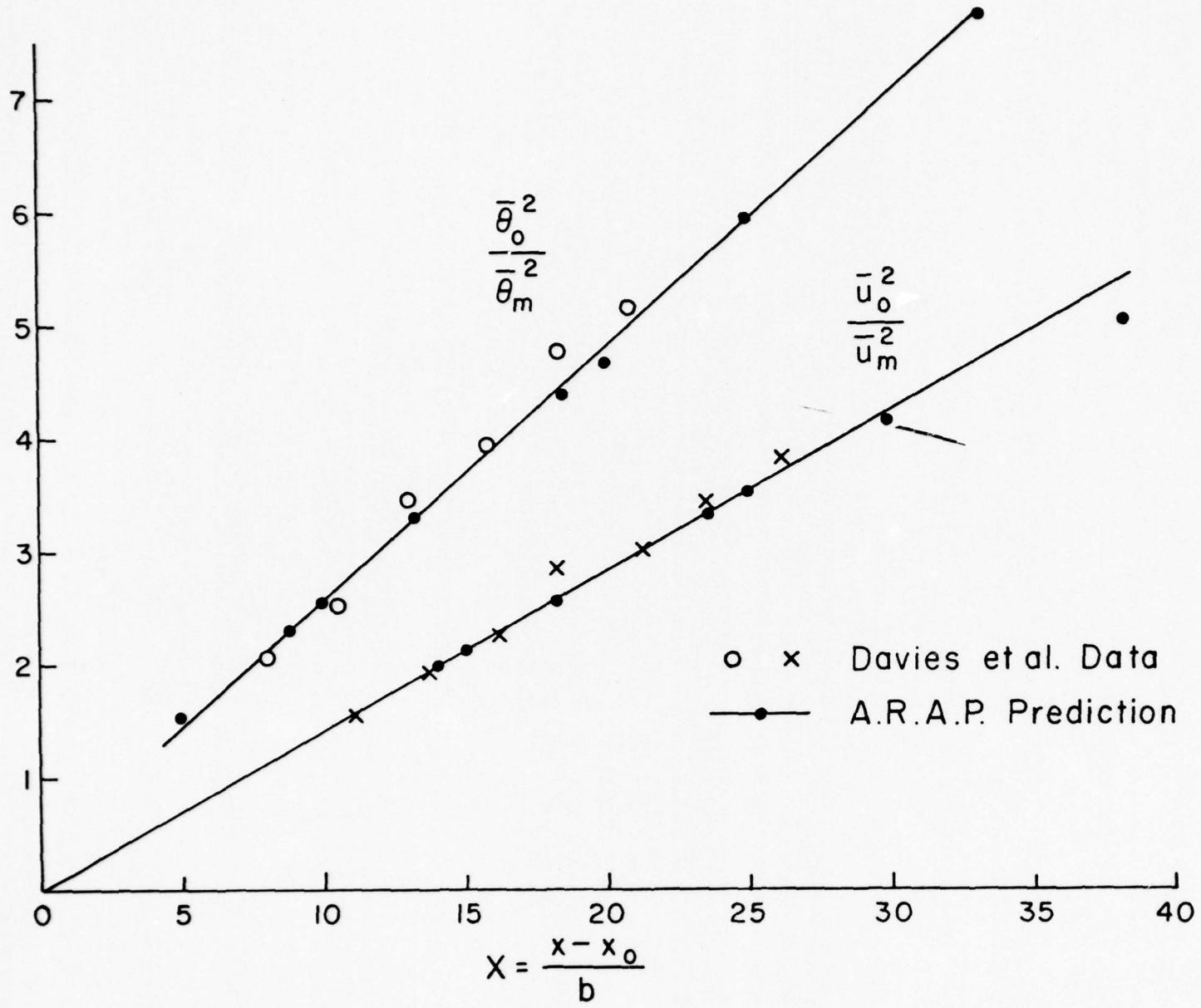

Figure 4. Decay of centerline velocity and temperature in a heated plane turbulent jet.

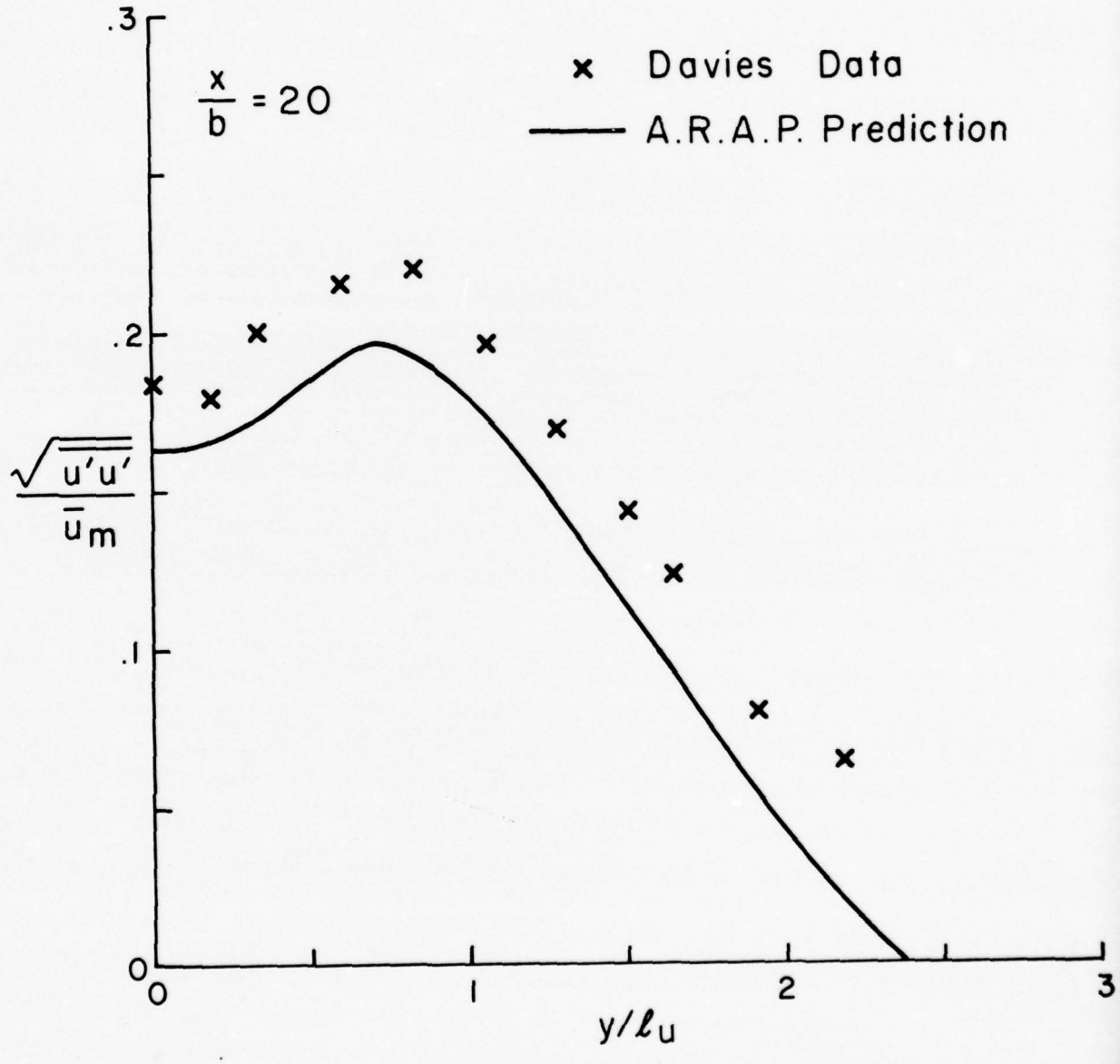

Figure 5. Mean turbulence intensity profiles in a heated plane turbulent jet.

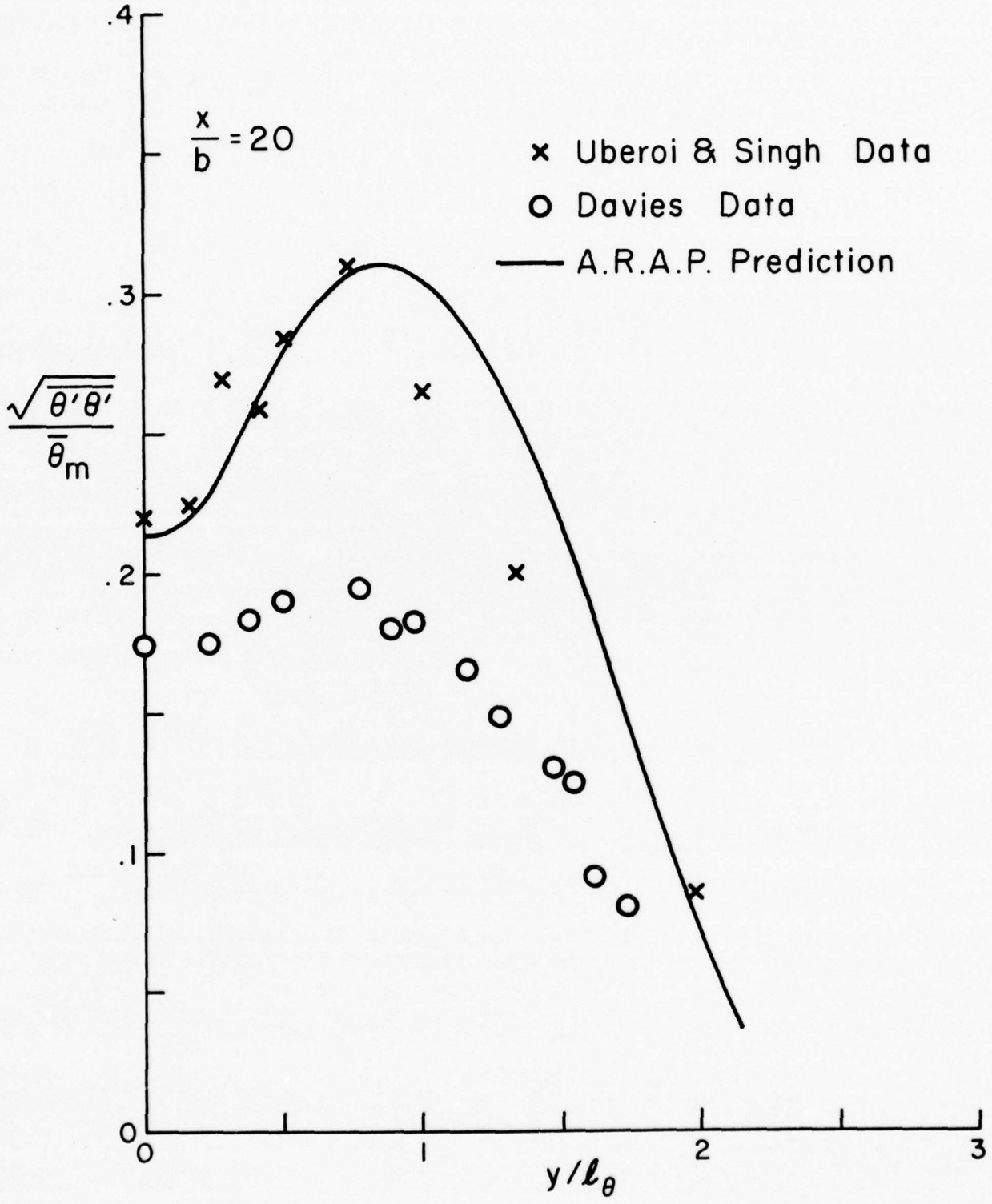

Figure 6. Temperature fluctuations in a heated plane turbulent jet.

and these are in much better agreement with our predictions, and are also more reasonable in shape considering the profile of the velocity fluctuations. The discrepancy between the measurements of Davies and Uberoi has to be investigated further. In both Figures 5 and 6, the predicted profile shape is in good agreement with the measurements.

Recent measurements in a two-species mixing layer have been reported by Konrad (Ref. 29). These measurements are part of a very elaborate and detailed study of this basic flowfield by the group under the direction of Prof. Roshko at Caltech. Konrad has made measurements of the mixedness correlation $\overline{\alpha'\beta'}/\bar{\alpha}\bar{\beta}$ or $\overline{\alpha'\alpha'}/\bar{\alpha}(1-\bar{\alpha})$ in a shear layer of velocity ratio = 0.38 and consisting of two streams of different species but the same density. Figure 7 shows a comparison of the RSL program predictions for the flowfield with the experimental measurements. There is good agreement in the central turbulent region of the flowfield. The theoretical predictions for the edge regions of the flow are not symmetrical, which is somewhat surprising and is believed to be due to the difficulty of accurately calculating the term $\overline{\alpha'\beta'}/\bar{\alpha}\bar{\beta}$ when $\bar{\alpha}$ or $\bar{\beta}$ is very small. This requires some further study. The disagreement between the theoretical predictions and the experiments may also be due to the intermittent nature of the flow in this region and the observed large structures in the turbulent flow. The theoretical models do not include intermittency effects at the present time.

All the above computations and those mentioned earlier have been carried out with basically the same set of model parameters. The results demonstrate that our second-order closure techniques correctly predict the mean flow and details of the turbulence correlations for a wide class of nonreacting flows and provide a level of confidence in the models and the programs. Similar tests have to be carried out for turbulent reacting flows to

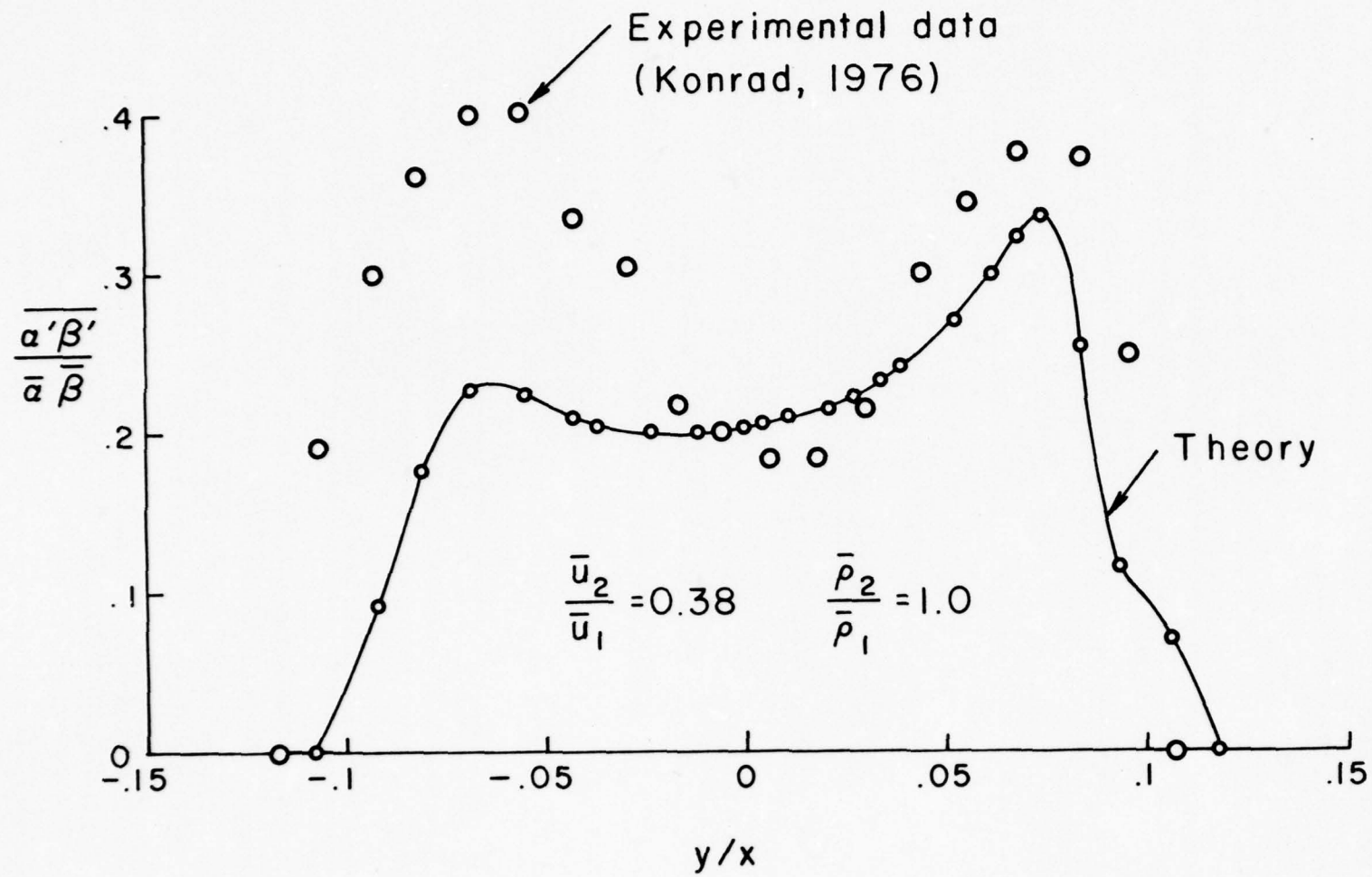

Figure 7. Profile of the mixedness correlation $\overline{\alpha'\beta'}/\bar{\alpha}\bar{\beta}$ in a shear layer.

verify the models developed for the scalar correlations. Recently, computational results have been presented for a hydrogen-air diffusion flame (Ref. 30) that correctly predict some of the important features of the flow. However, many more such tests remain to be made to thoroughly check the models and the programs.

IV. CHEMICAL LASER FLOWFIELD COMPUTATIONS

The A.R.A.P. turbulent reacting shear layer (RSL) program has been used to study the mixing and chemical reactions in the initial region of the flowfield of a supersonic DF chemical laser. The flow parameters and the initial geometry for the studies are shown in Figure 8. The design data corresponds to the MESA IV slit nozzle built by Rocketdyne, and was provided by the Air Force Weapons Laboratory. The flow parameters were originally for a HF chemical laser system. For our studies we simply replaced the H_2 by D_2 and maintained all the other flow parameters at the same level. The nozzle wall boundary layers and the dead water regions at the nozzle exits are ignored in these studies. The analysis of the dead water region is particularly difficult as recirculating flows are likely to be present and elliptical flow equations have to be solved to properly characterize the region. The effect of the initial nozzle wall boundary layers, however, can be included in the computations without too much effort in the future.

The initial profiles of the mean variables are taken to be smooth profiles of width .025 cm (10% of the total width) between the specified values on the nozzle centerlines. The computational region is from the centerline of the D_2 nozzle to the centerline of the fluorine + helium stream. Suitable boundary conditions are used at these symmetry planes. The turbulence correlations $\overline{u'u'}$, $\overline{v'v'}$, $\overline{w'w'}$, and $\overline{u'v'}$ are specified at the initial station to begin the computations. Typically, a spot of turbulence of variable amplitude and with $\overline{u'u'} = \overline{v'v'} = \overline{w'w'} = 2\overline{u'v'}$ is used at the nozzle exit in the mixing region between the two streams. The effects of varying the initial turbulence amplitude and the distribution of the total turbulence kinetic energy q^2 among the three normal stresses has been studied. The mixedness correlation $\overline{\alpha'\beta'}/\bar{\alpha}\bar{\beta}$ was also specified as nonzero at the initial station in some of the runs.

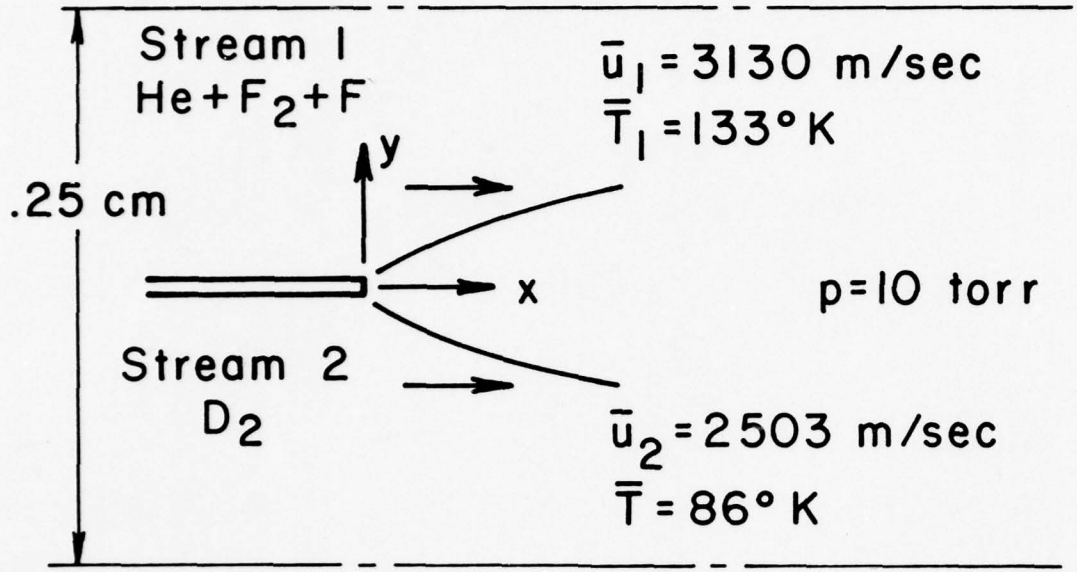

Figure 8. Flow configuration.

In these runs, this correlation was set at -1.0 across the entire profile at $x = 0$,, and then allowed to develop according to its transport equation. For initially unmixed streams of reactants α and β , -1 is the proper value at the initial station, for α and β do not coexist at any point and are thus perfectly anti-correlated. However, the initial value of this correlation is not of crucial importance. In identical runs with $\overline{\alpha'\beta'}/\bar{\alpha}\bar{\beta} = 0$ or -1 at the initial station, the correlation reaches the same downstream value in a very short distance, as would be expected in a marching solution procedure. The effect of the initial conditions is wiped out in a distance of a few relaxation lengths of the flowfield. All the other turbulence correlations are set at zero at the initial station. The pressure is maintained constant at the specified cavity pressure throughout the flowfield.

The primary objective of our research program was to parametrically study the effect of various turbulence flow parameters — turbulence kinetic energy q^2 , turbulence distribution or isotropy, turbulence macro-scale Λ , and the turbulence-chemistry interaction effects — on the initial activation region of the flowfield of a supersonic DF chemical laser. Concentrating on the initial excitation reactions for the production of excited DF(v) species, a 16-step reaction scheme was used for the majority of the test runs of the program reported in this report. This reaction scheme was specified by AFWL and DARPA personnel and is listed in Table 1. This set of reactions is only a small subset of the complete reaction scheme as proposed by Cohen (Ref. 31). The excitation reactions up to the fourth vibrational level for DF have been included. The laser deactivation reactions have not been considered in our studies. Toward the end of our research program, some modifications and additions were made to the reaction scheme listed in Table 1 to evaluate the sensitivity of the computations

to the selected reaction scheme. The changes were to replace the DF0 in reactions 5-8 by $\sum_{v=0-4} DF(v)$ and to add the deactivation reactions with helium. The modified reaction scheme used in some of the runs is listed in Table 2. The use of the more complete reaction scheme led to very minor changes in the program predictions.

The results of our studies are discussed in the next section. The computations using the reaction scheme of Table 2 will indicate this fact. All other runs have been run using the 16 reaction scheme detailed in Table 1.

V. RESULTS AND DISCUSSION

A majority of current HF and DF chemical laser systems operate at cavity pressures of the order of 10 torr. The flow Reynolds number of these devices is of the order of 10^3, and turbulent transport is unimportant except in a small initial region after the nozzle exit where the turbulence is the decaying turbulence field left over from the nozzle wall boundary layers and the recirculation regions at the nozzle exits. Chemical laser configurations now being investigated for future systems are expected to operate at higher cavity pressures and in flow regimes where turbulent transport processes will be more important. The use of boundary layer trips to produce turbulent boundary layers in the nozzles has led to some improvement in laser performance, but some of the observed effects are not easily explained. In some cases a decrease in laser performance has resulted from attempts to introduce turbulence into the flow. The effects of various turbulence parameters on the mixing and reaction in the chemical laser are quite complex.

The flow parameters of the DF chemical laser under study have been shown in Figure 8. The cavity pressure in the actual system is 10 torr, and the flow Reynolds number is about 5×10^3. The effect of the following four turbulence parameters on the formation of excited DF species in the initial region has been studied.

1. Initial disturbance amplitude $\overline{u'u'}_{init}$ with isotropic distribution $\overline{u'u'} = \overline{v'v'} = \overline{w'w'}$.

2. Turbulence distribution with constant turbulence kinetic energy $q^2 = \overline{u'u'} + \overline{v'v'} + \overline{w'w'}$.

3. Turbulence macroscale Λ .

4. Inclusion or neglect of the mixedness correlation $\overline{\alpha'\beta'}/\bar{\alpha}\,\bar{\beta}$ in the chemical source terms.

Similar calculations have also been performed for a cavity pressure of 100 torr with the same flow geometry to study the effect of raising the operating pressure and the flow Reynolds number. The results for 10 torr cavity pressure, the normal operating conditions, are discussed first followed by the results for 100 torr pressure.

Laser Cavity Pressure = 10 Torr

The behavior of the maximum value of the $\overline{u'u'}$ correlation at different downstream axial stations is shown in Figure 9. The figure shows the results for calculations started with two different initial levels of turbulence, $\overline{u'u'}_{init} = .004$, $.04$. The turbulence distribution is isotropic and the macroscale has the normal value $\Lambda = .05\ (y_{.75} - y_{.25})$, where $y_{.75}$ and $y_{.25}$ are the values of the normal coordinate where $\bar{u} - \bar{u}_2/\bar{u}_1 - \bar{u}_2$ is .75 and .25, respectively. The turbulence field here is just the rapidly decaying turbulence left over from the nozzle wall boundary layers and the dead water recirculating regions at the nozzle exit. The initial turbulence level can be increased by the use of boundary layer trips of various designs. Due to the low flow Reynolds number at $p = 10$ torr , the turbulence decays very rapidly, and a laminar transport analysis would appear to be justified for most of the flowfield. However, as the figure shows, in this initial region the turbulence level at a point is strongly dependent on the amplitude of the initial disturbance, and it is shown later that there are significant differences in, for example, DF(2) formation as a function of the initial turbulence amplitude.

Figures 10 and 11 present the results with and without the inclusion of turbulent scalar correlations, like the mixedness

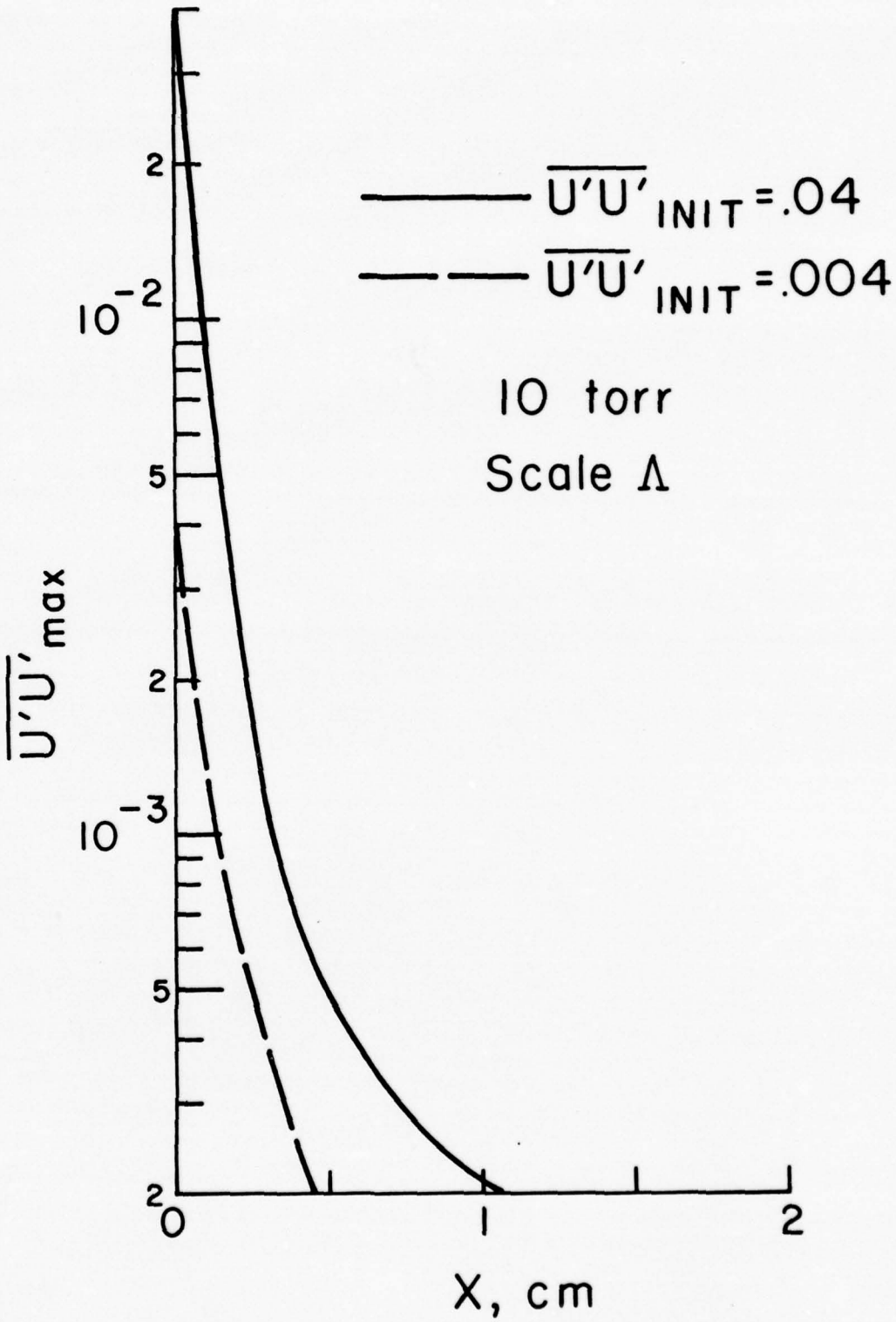

Figure 9. Axial decay of turbulence.

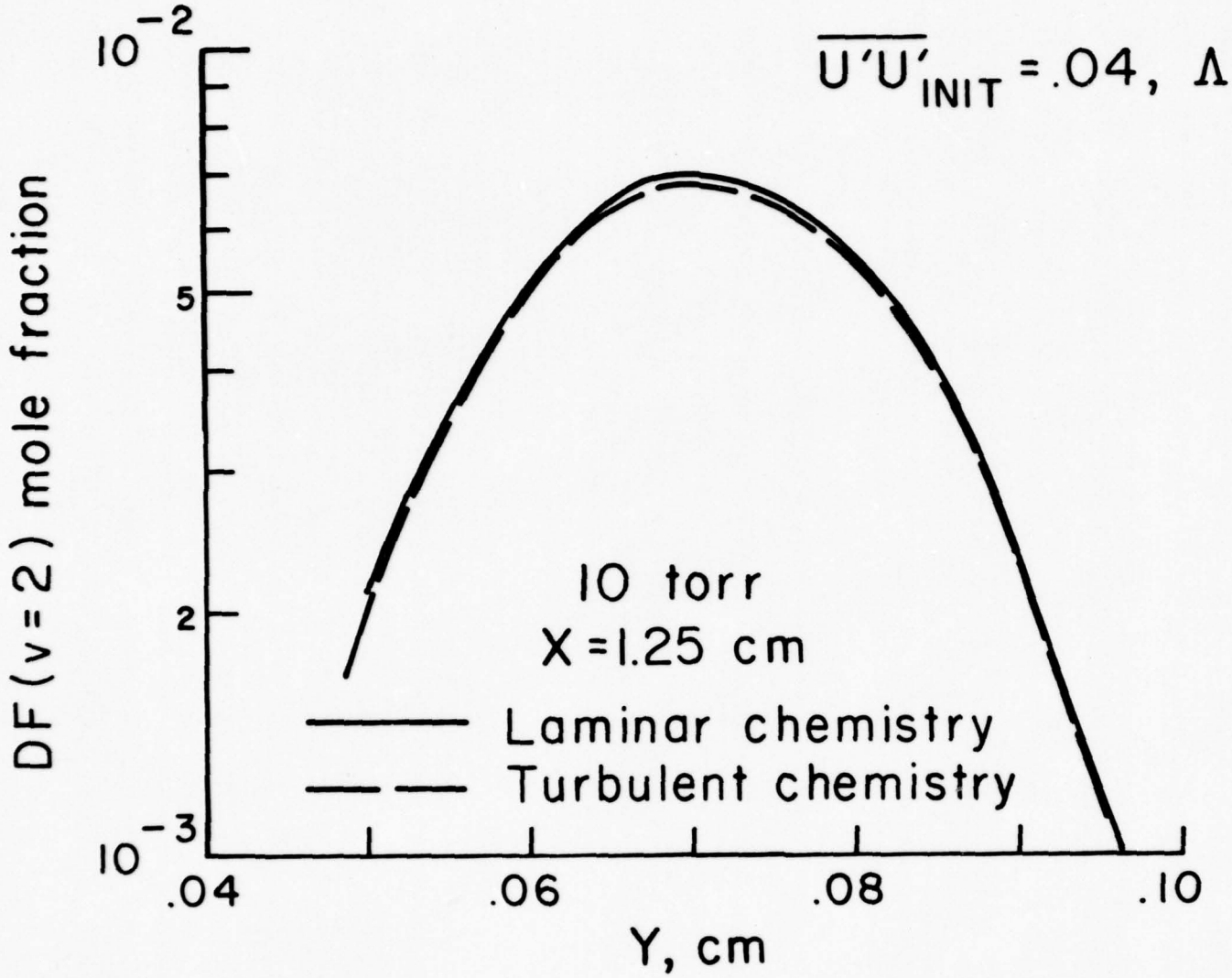

Figure 10. Comparison of DF(2) production with and without the inclusion of the turbulent scalar correlations in the chemical source terms. X = 1.25 cm

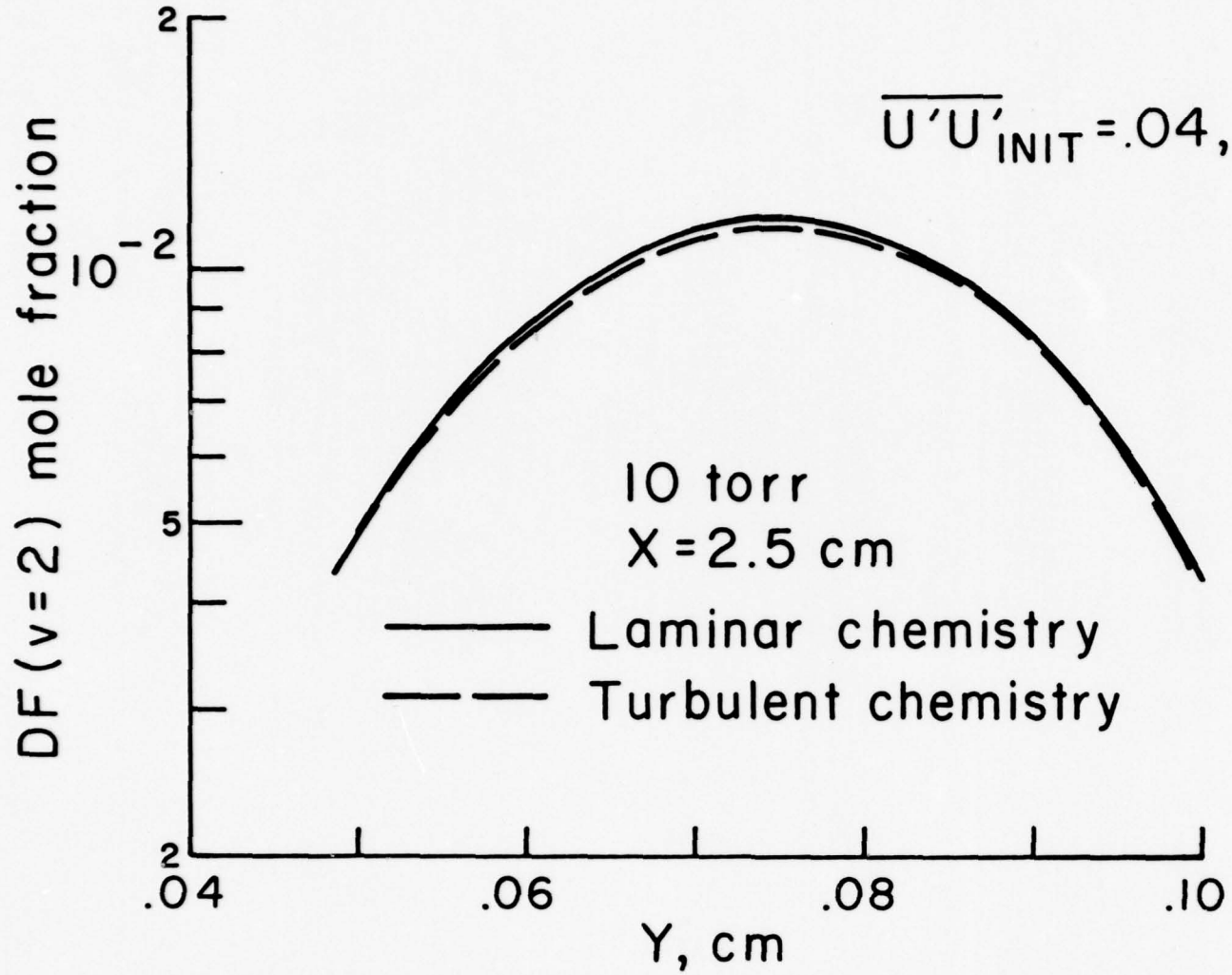

Figure 11. Comparison of DF(2) production with and without the inclusion of the turbulent scalar correlations in the chemical source terms. X = 2.5 cm

correlation $\overline{\alpha'\beta'}/\bar{\alpha}\bar{\beta}$, in the chemical source terms. The concept can be illustrated by the following simplified problem. Consider the expression for the rate of change of a species α , due to chemical reactions in a turbulent flow. Assume a simple one-step reaction $\alpha + \beta \rightarrow \gamma$. Then,

$$\frac{d\alpha}{dt} = -k\alpha\beta$$

$$\frac{d\bar{\alpha}}{dt} = -\bar{k}\bar{\alpha}\bar{\beta} - \overline{k\alpha'\beta'} + \bar{\alpha}\overline{k'\beta'} + \bar{\beta}\overline{k'\alpha'} + \overline{k'\alpha'\beta'}$$

Many of the previous studies of turbulent reacting flows neglect the group of terms within the brackets and simply use

$$\frac{d\bar{\alpha}}{dt} = -\bar{k}\bar{\alpha}\bar{\beta}$$

for the chemical source term calculation. This is analogous to the source term for laminar flow, and we designate this procedure as the "laminar chemistry" approximation. Another error in this approximation is the evaluation of $\bar{k}$; usually one takes $\bar{k} = k(\bar{T})$ which is only true for laminar flow. In the "turbulent chemistry" runs, $\bar{k}$ is evaluated from the pdf for "typical eddy" model runs and from second-order accurate expansions of the Arrhenius rate expression for "secondary" model runs, and all the terms in the brackets are included in the evaluation of the chemical source term. In the current studies on the DF chemical laser reported here the "secondary" model has been used for the higher-order scalar correlations. Further, as the temperature changes in the laser flowfield are quite small, temperature fluctuation (and therefore, k') effects have been neglected. Therefore, in the current studies, the "turbulent chemistry" formulation corresponds to the use of the expression

$$\frac{d\bar{\alpha}}{dt} = -k\bar{\alpha}\bar{\beta}\left(1 + \frac{\overline{\alpha'\beta'}}{\bar{\alpha}\bar{\beta}}\right)$$

and the "laminar chemistry" approach involves the neglect of the mixedness correlation.

The computations in Figures 10 and 11 show the transverse profiles of DF(2) at distances 1.25 cm and 2.5 cm downstream of the nozzle exit. The results for the other vibrational levels are similar. The initial disturbance was isotropic and of amplitude $\overline{u'u'} = .04$ and scale Λ. The results show that for $p = 10$ torr, the inclusion of the fluctuating chemical source terms has a negligible effect on the formation of DF(v). The turbulence-chemistry interaction effects are very small for these conditions. It is shown later that for larger scale disturbances, there are some significant turbulence-chemistry interactions even at $p = 10$ torr.

The effect of various initial turbulence levels on DF(2) formation is shown in Figures 12 and 13. Figure 12 shows the profiles of DF(2) at 2.5 cm axial distance downstream of the nozzle exit for laminar flow and $\overline{u'u'}_{init} = .004$ and $.04$. The integrated DF(2) formation in the normal direction is shown in Figure 13 as a function of the axial position. As remarked earlier, due to the rapid decay of the turbulence the actual turbulence level in the initial region is strongly dependent on the initial disturbance level and results in significant changes in the formation of the excited species. Higher initial disturbances predict the formation of larger amounts of DF(2) and thus should lead to improved laser performance. Deactivation reactions, of course, must be included in the analysis to correctly predict the laser performance.

The use of boundary layer trips in the nozzles would introduce initial disturbances of variable amplitude, isotropy, and

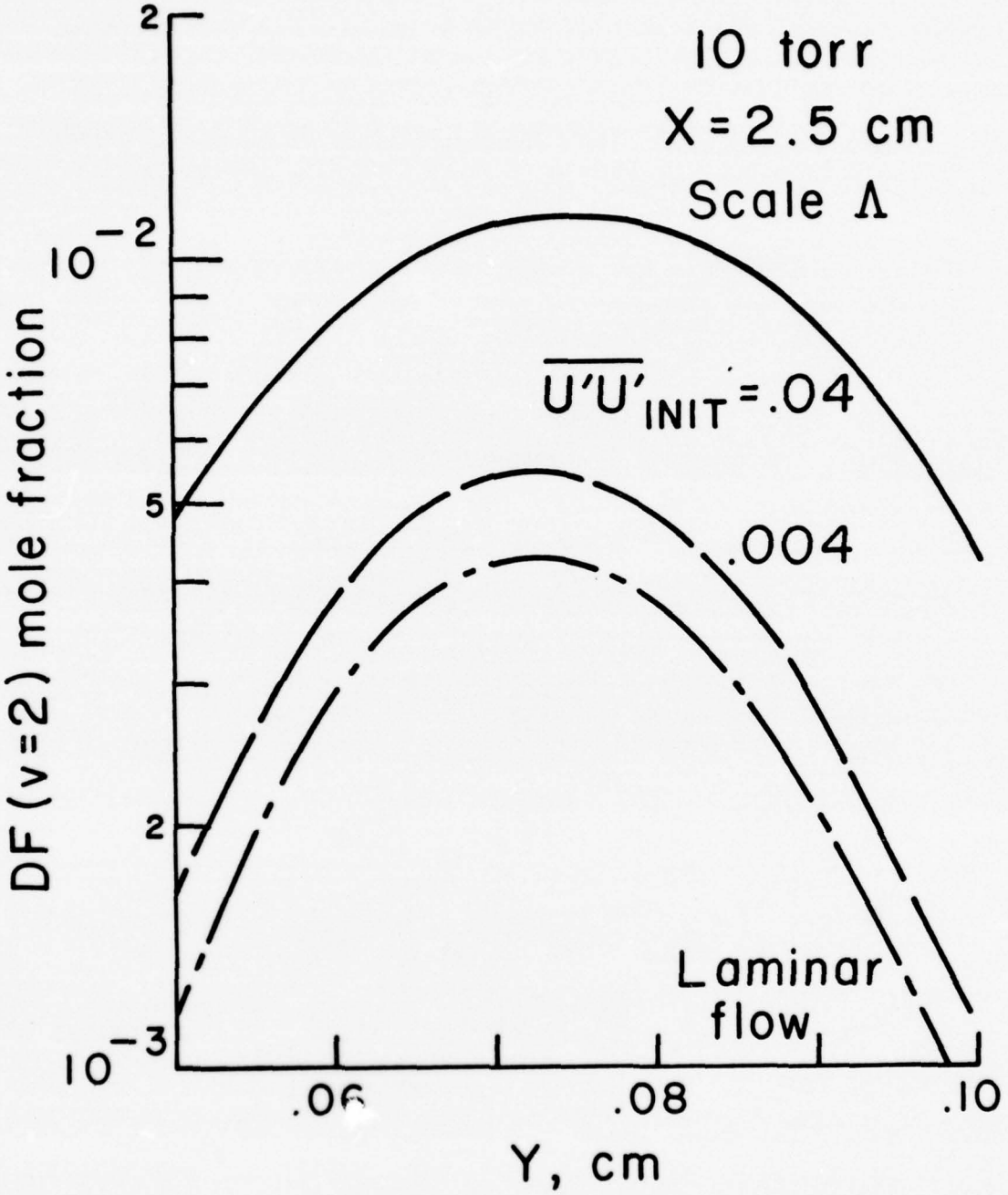

Figure 12. Effect of various initial turbulence levels on DF(2) formation.

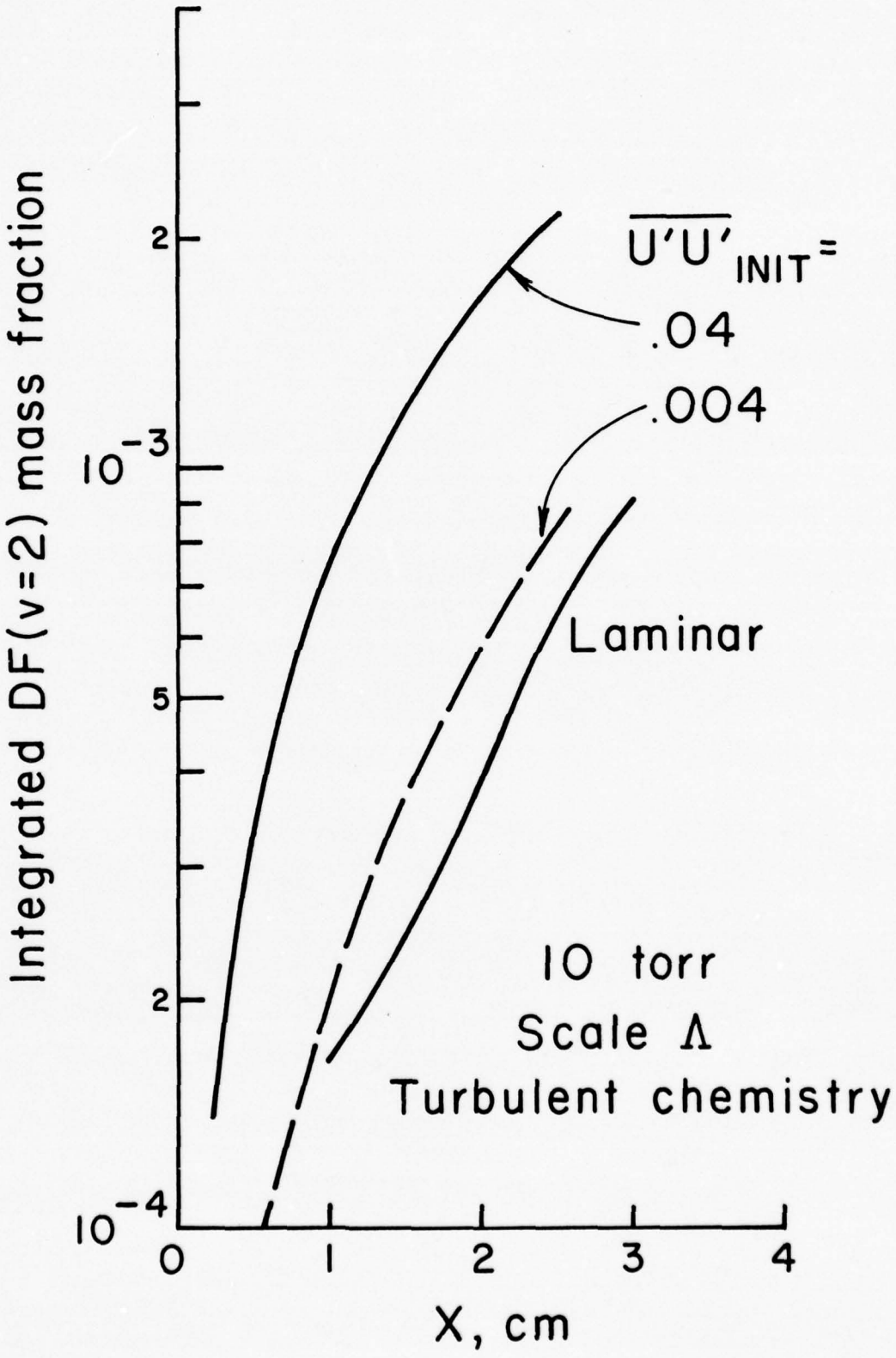

Figure 13. Effect of various initial turbulence levels on integrated DF(2) formation.

scale. The effects of isotropy and turbulent macroscale variation have been studied, and are discussed next.

The effect of turbulence isotropy was investigated by the following three runs. The turbulent kinetic energy q^2 was kept constant at 0.12 and the scale Λ was used. The three distributions used are tabulated below, and correspond

$\overline{u'u'}$	$\overline{v'v'}$	$\overline{w'w'}$
.03	.06	.03
.04	.04	.04
.06	.03	.03

to typical limiting distributions that are observed in a variety of atmospheric turbulent flows. The results for $p = 10$ torr are shown in Figure 14 for two axial stations. There are small differences very close to the nozzle exit, but in the region of interest for the laser cavity (~ 2 cm) there is virtually no effect of the initial isotropy characteristics of the disturbances.

The current version of the reacting shear layer (RSL) program uses a constant, algebraically specified turbulence macroscale Λ across the entire flow region in the normal direction. The scale is based either on the mean axial velocity profile or on the profile of the turbulence kinetic energy. In all the laser calculations discussed here, the scale is based on the mean velocity profile and $\Lambda = 0.5\ (y_{.75} - y_{.25})$. We are currently engaged in the development of a transport equation for the turbulence macroscale for compressible flows using the formulation for a two-point correlation function. Calculations have been performed to show the effect of scale variation ranging from 0.7 Λ to 2.0 Λ. The scale modification parameter,

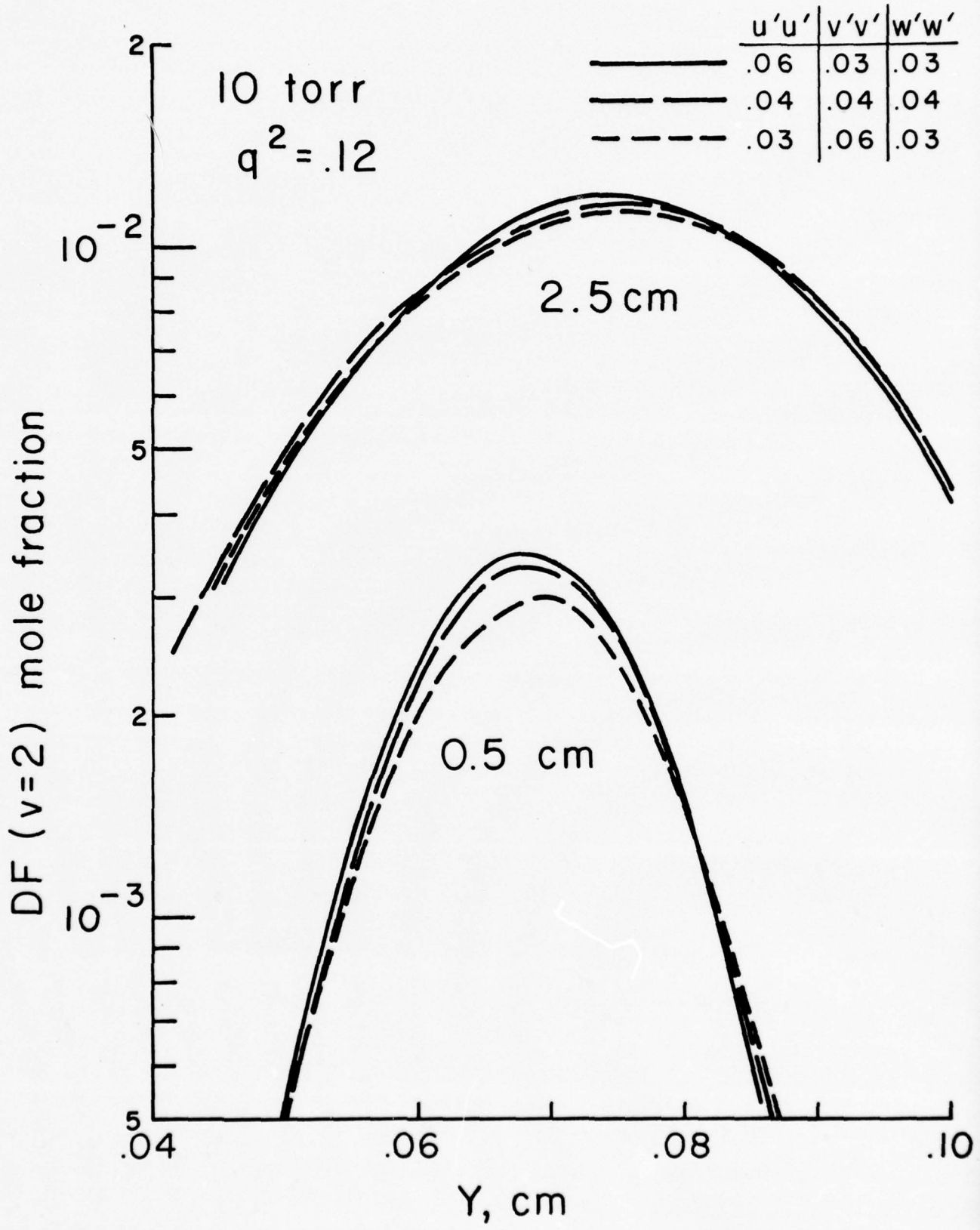

Figure 14. Effect of initial turbulence distributions on DF(2) formation.

i.e., 0.7 or 2.0, remains constant in the program calculations although in the actual flow if a larger scale disturbance were introduced at the initial station, it would adjust to the local flowfield conditions in some characteristic relaxation time of the order of Λ/q . Figure 15 shows the effect of doubling the scale on the transverse profile of DF(2) at the axial station $X = 2.5$ cm . The result is not surprising as the larger scale will result in increased transverse mixing and a more uniform profile. The calculations were done using the turbulent chemistry formulation. It has been shown before that for 10 torr runs with scale Λ , the turbulent chemistry and the laminar chemistry results are virtually identical. However, when the scale is increased to 2Λ, there are significant differences. Figure 16 shows the results for 10 torr, 2Λ runs using laminar and turbulent chemistry at $X = 2.5$ cm . Figure 17 presents the integrated DF(2) mass fraction as a function of the axial position for the same conditions. The comparison shows substantial differences between the laminar and turbulent chemistry formulations, and significant errors can result from the neglect of the turbulence-chemistry interaction. The behavior of the species mixedness correlation $\overline{\alpha'\beta'}/\bar{\alpha}\bar{\beta}$ for 10 torr and scales Λ and 2Λ is shown in Figure 18. In the turbulent chemistry runs we normally start with an initial value of the correlation of -1 across the mixing layer. For scale Λ , the mixedness rapidly drops to negligible values in line with the behavior of the velocity turbulence correlation, and this is the reason why Figures 10 and 11 showed virtually no difference between the laminar and turbulent chemistry calculations. When the scale is increased to 2Λ, the mixedness correlation has fairly substantial values for the entire flowfield and this leads to significant differences between the laminar and turbulent chemistry calculations.

The overall effect of scale changes on laser performance can be estimated by comparing the integrated DF(v) mass fractions across the normal profile. Figure 19 presents the results for

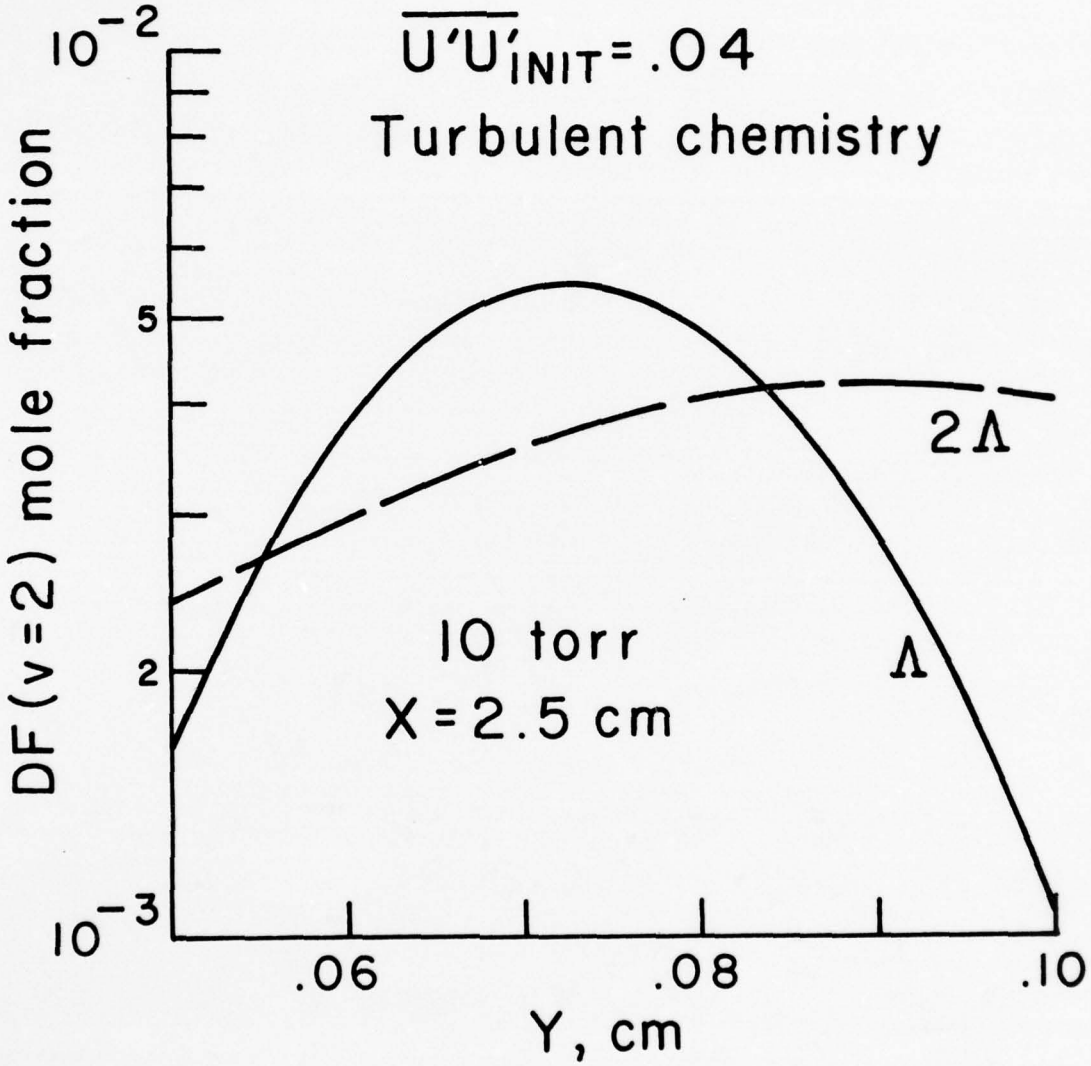

Figure 15. Effect of turbulence macroscale on DF(2) production.

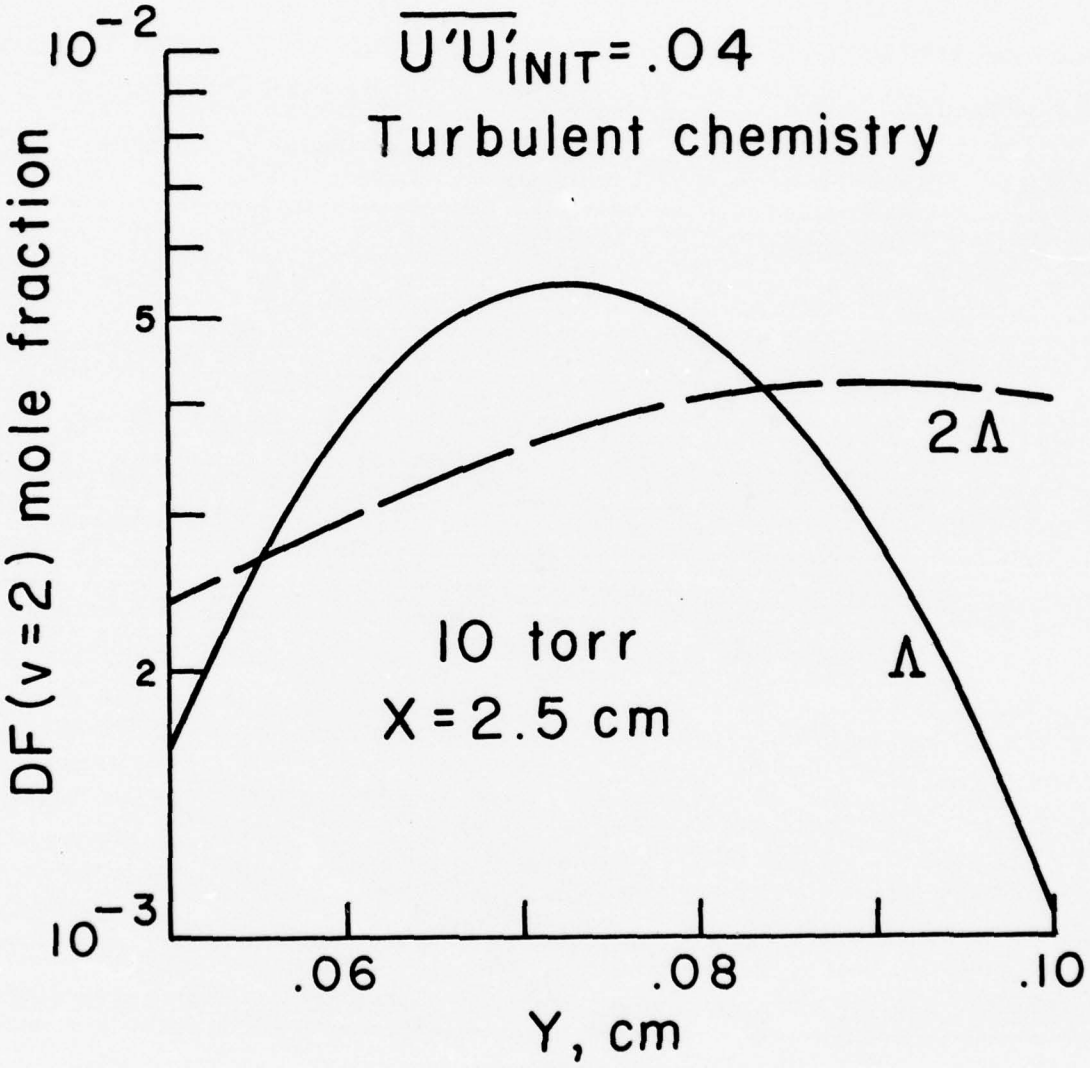

Figure 15. Effect of turbulence macroscale on DF(2) production.

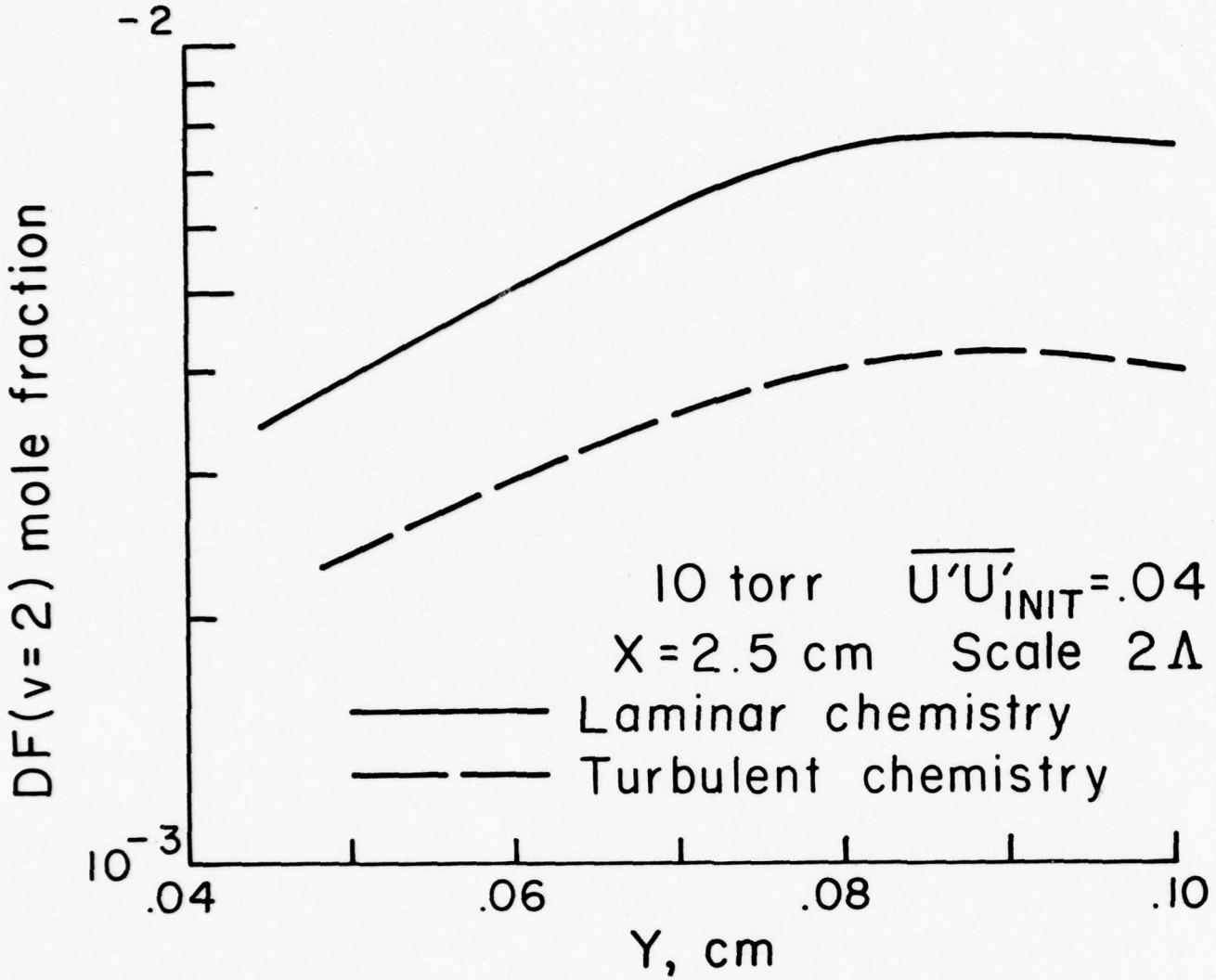

Figure 16. Comparison of laminar and turbulent chemistry formulations on DF(2) formation.

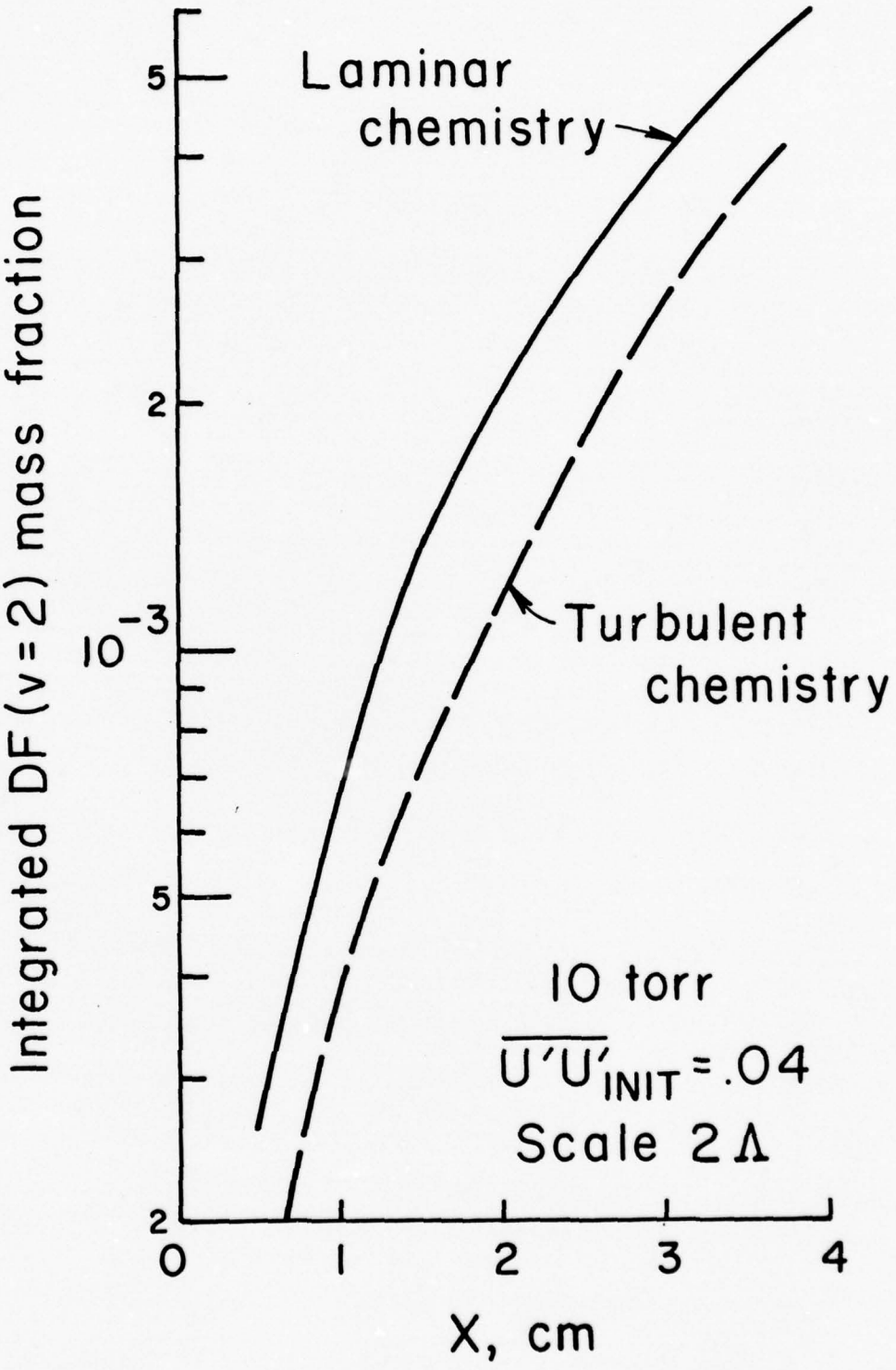

Figure 17. Comparison of laminar and turbulent chemistry formulations on integrated DF(2) formation.

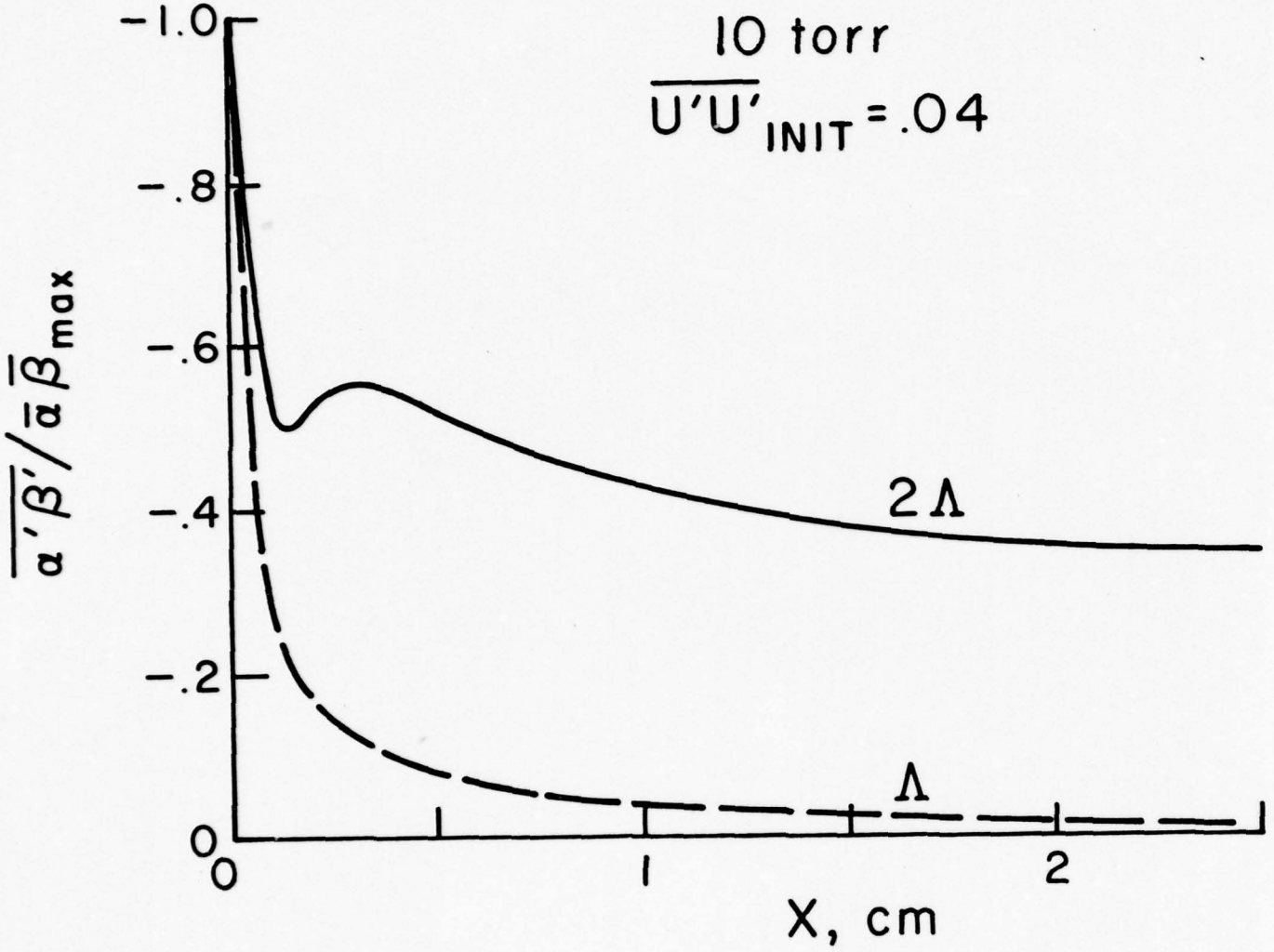

Figure 18. Behavior of the mixedness correlation for two different scales.

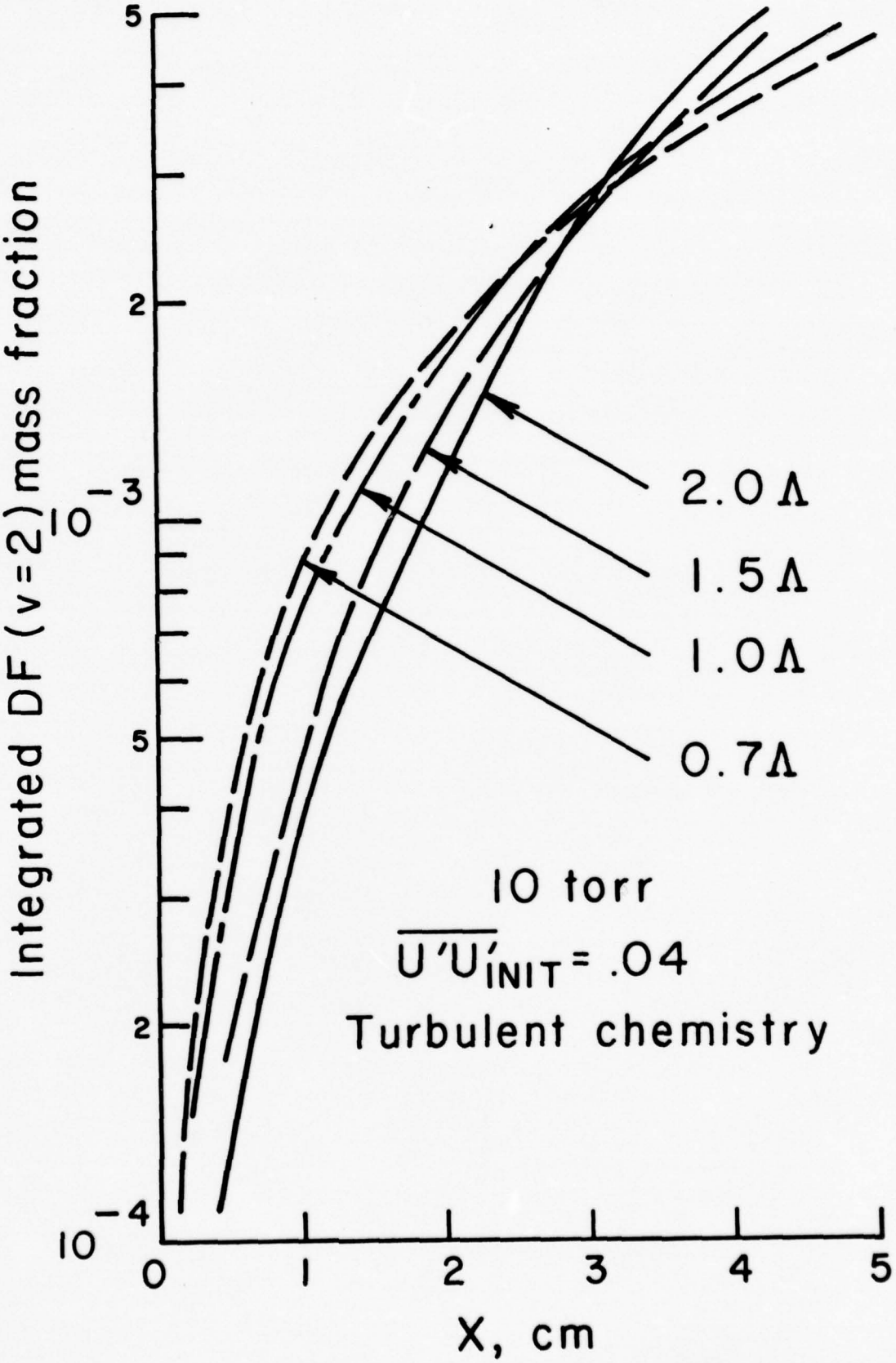

Figure 19. Integrated DF(2) formation for four different turbulence scale parameters.

the four different scale parameters. The results show that in the initial region of the flow (up to $X = 2$ cm) there are substantial differences in total DF(2) formation, with a smaller scale leading to increased laser performance. Further downstream, the scale effect is smaller in magnitude, and a crossover of the predicted curves is seen indicating improved performance for the larger scales.

These results for the 10 torr cavity pressure DF laser show the significant effects of the two turbulence parameters — initial disturbance amplitude and the turbulence macroscale — on the performance of the laser. Different combinations of turbulence amplitude and scale could lead to improvement or degradation of the laser performance and may, in part, explain the discrepancies in experimental studies. Of course, as remarked earlier, our studies must be repeated with a more complete set of reactions including laser radiation effects to enable direct comparison to experiments and to make the results applicable to the actual laser system.

The important results for the 10 torr cavity pressure DF laser are summarized in Figure 20. The integrated DF(2) mass fraction at $X = 1.25$ cm is plotted as a function of the initial turbulent kinetic energy q^2 , for a number of different scale runs. There are only five data points on the graph, but the behavior of DF(2) formation with q^2 can be reasonably expected to have the trends indicated in the figure. If the nozzle wall boundary layers are tripped by gas injection through the nozzle walls, increases in turbulence may be accompanied by increases in the scale, and it may be hypothesized that for increased blowing one follows the path indicated on the figure. There is an initial improvement in DF(2) formation (and laser performance), but further increase in blowing results in an adverse effect on the total DF(2) production due to the increased turbulence scale. The above is merely a hypothetical example of

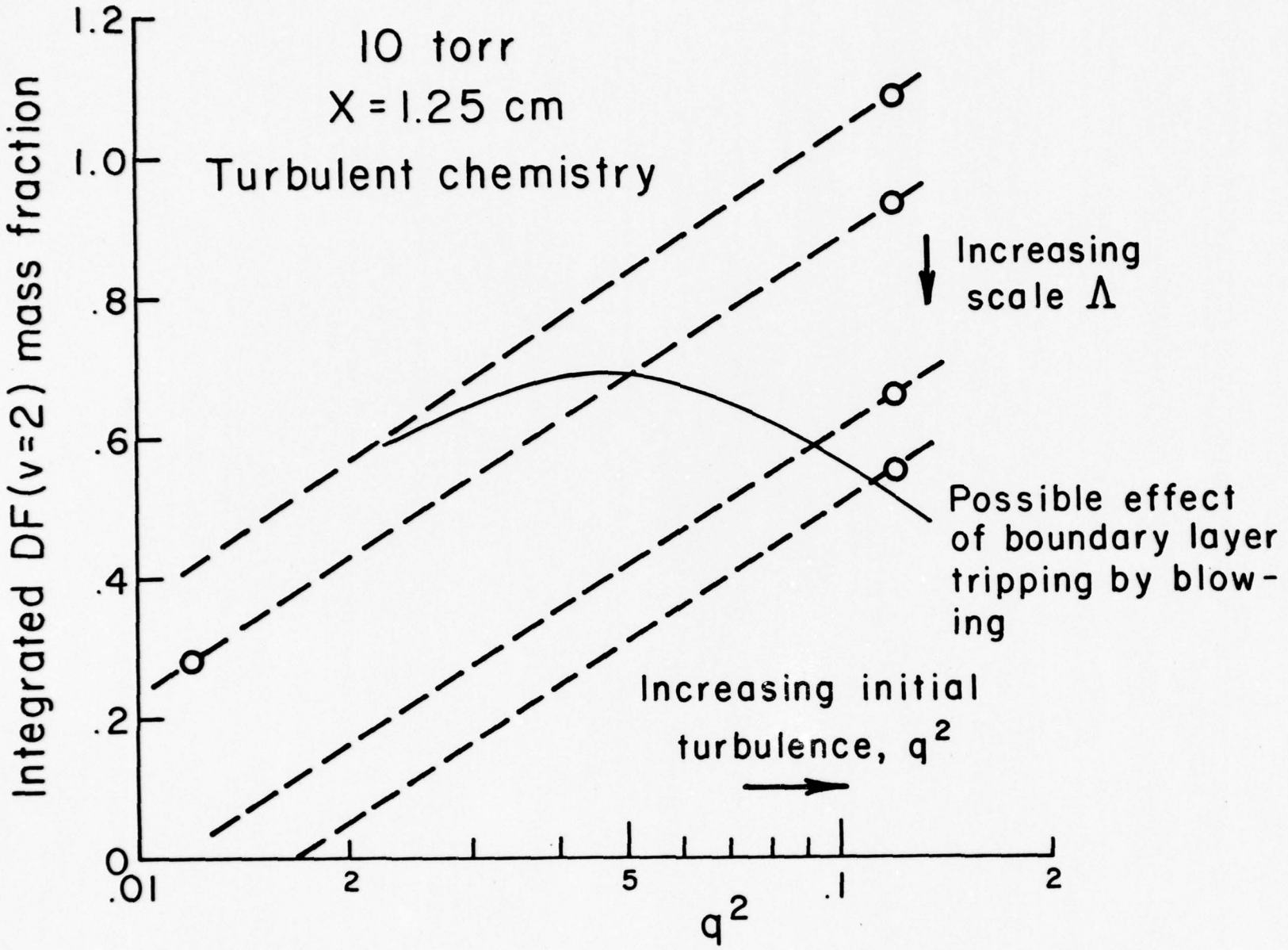

Figure 20. Schematic diagram showing decrease in DF(2) production due to boundary layer tripping by blowing.

the kind of effects that may be encountered in attempts to modify the turbulence parameters in the chemical laser flowfield. There is very little information available on the scales and intensities of turbulence produced by various trip mechanisms and some investigation of this should be carried out. Our program calculations clearly demonstrate the effects of these turbulence parameters on the production of vibrationally excited DF species in the initial region of the chemical laser.

Laser Cavity Pressure = 100 Torr

The pressure recovery of supersonic mixing chemical lasers could be improved by operating at higher cavity pressures. However, collisional deactivation also increases at higher pressures and more rapid mixing and reaction is necessary to maintain or improve the laser performance. Turbulence provides a convenient mechanism to increase the rate of mixing. At higher cavity pressure the flow Reynolds number is higher and, therefore, it is possible to operate in a regime where turbulent transport processes would be dominant. The reacting shear layer program has been used to study the effects of raising the cavity pressure to 100 torr.

The behavior of the velocity turbulence correlations is shown in Figure 21. The flow Reynolds number is of the order of 5×10^4, and the turbulence approaches an equilibrium value in a distance of a few centimeters. The initial amplitude of $\overline{u'u'}$ does not affect this equilibrium value and, as will be shown later, does not significantly affect the total DF(2) formation. The behavior of $\overline{u'u'}_{max}$ for $p = 10$ torr is also shown on the figure for comparison.

Figure 22 shows the comparison of "laminar chemistry" versus "turbulent chemistry" at $p = 100$ torr for two axial stations. All the 100 torr calculations use the normal turbulence macroscale Λ. The computations show very substantial differences in the

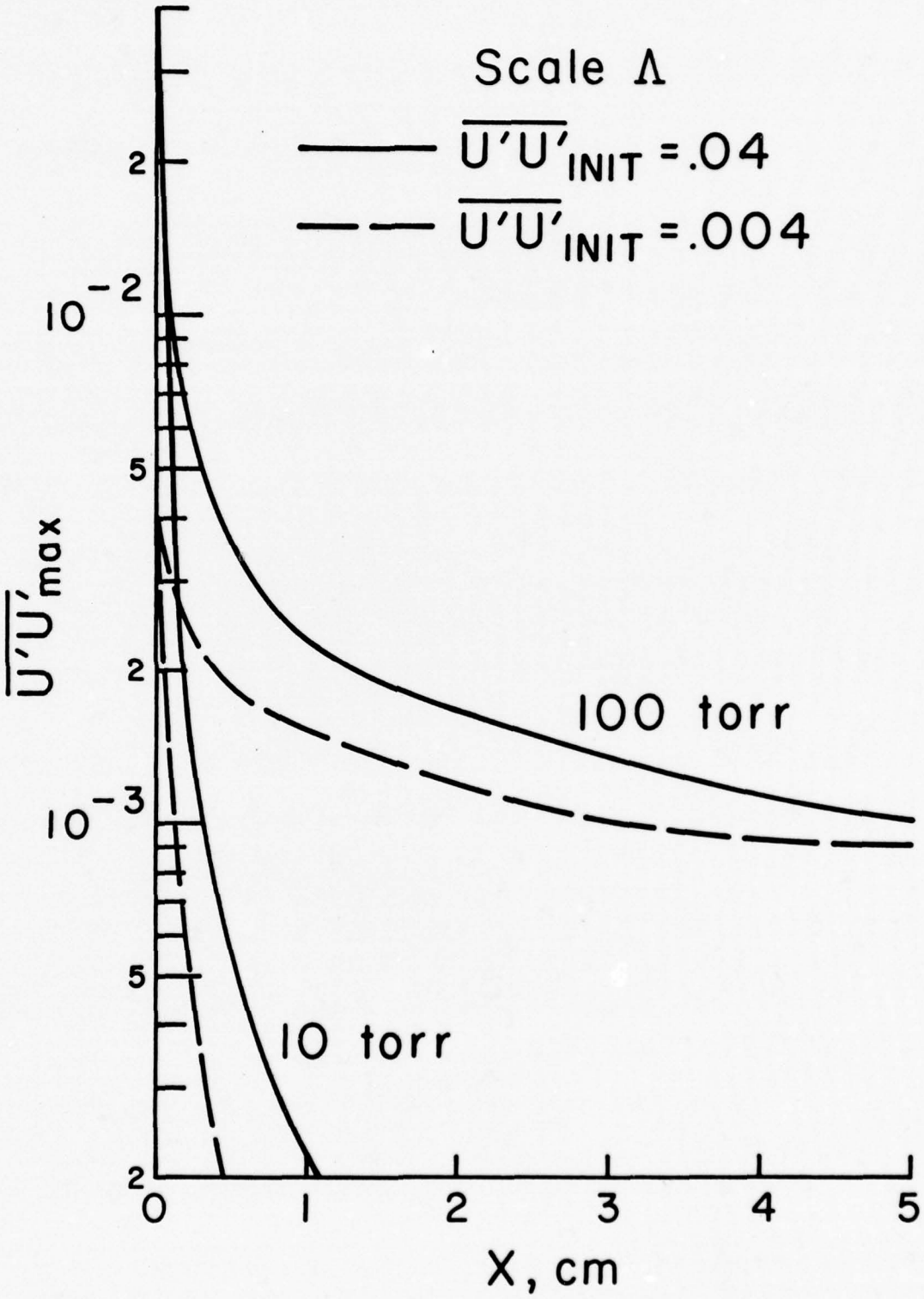

Figure 21. Effect of cavity pressure on the axial behavior of turbulence

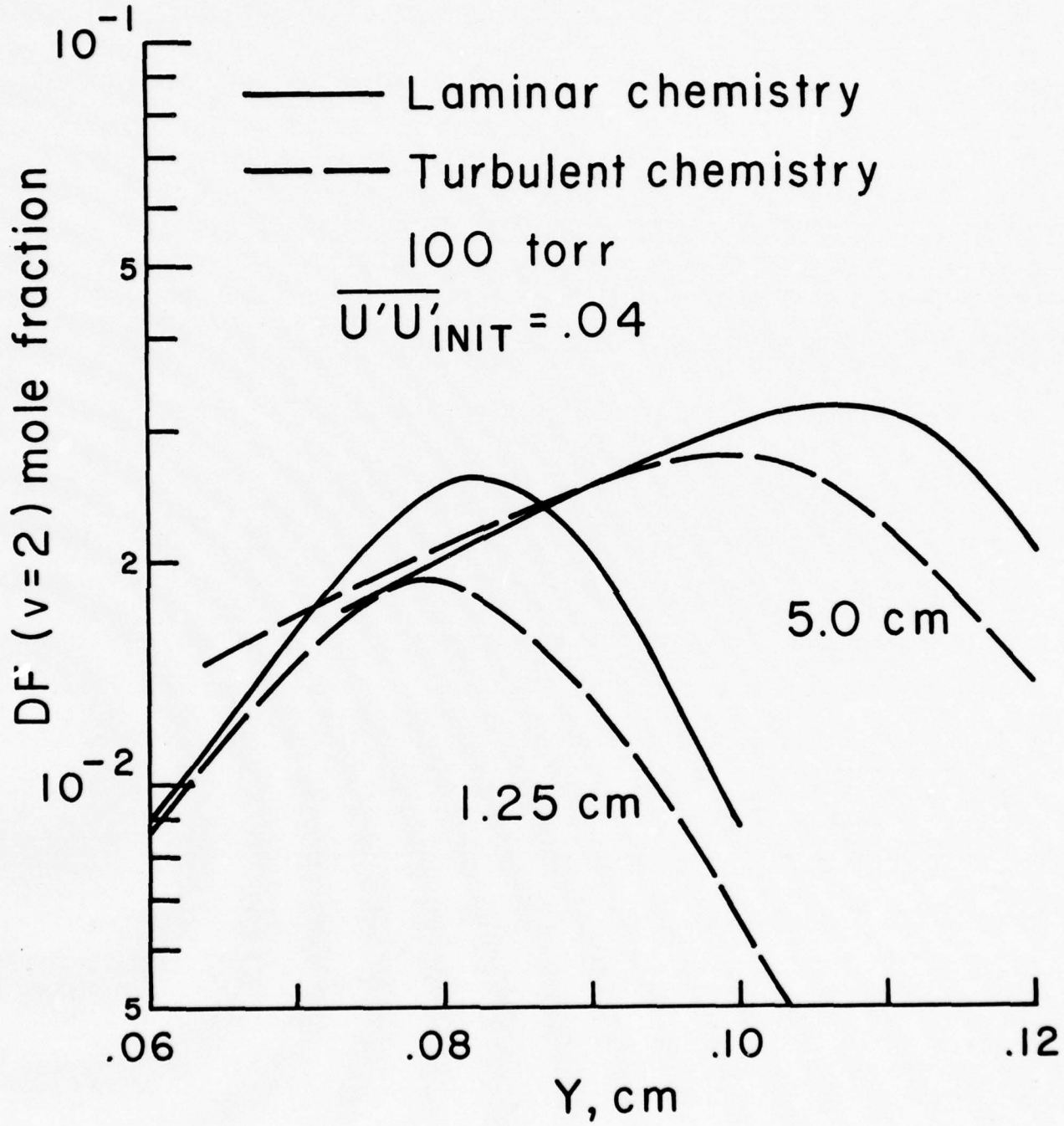

Figure 22. Comparison of DF(2) production with and without the inclusion of the turbulent scalar correlations in the chemical source terms.

DF(2) formation. The effect of the species fluctuations is to reduce the rate of the reaction below that based on the means alone, for the species are not mixed on the molecular scale to the extent predicted by the time-average concentrations. For very rapid reactions the species mixedness correlation $\overline{\alpha'\beta'}/\bar{\alpha}\bar{\beta}$ approaches -1, so that the rate of reaction could be orders of magnitude smaller than that predicted by $\bar{k}\bar{\alpha}\bar{\beta}$. The effect of the temperature (or reaction rate) fluctuation terms is more complicated for it depends on whether they are positively or negatively correlated with the various species. However, the figure clearly demonstrates that significant errors can result from the neglect of the turbulence-chemistry interaction. The behavior of the species mixedness correlation for the 100 torr runs is shown in Figure 23. The computations normally start with an initial value of $\overline{\alpha'\beta'}/\bar{\alpha}\bar{\beta} = -1$ across the mixing layer. Some runs were started with the correlation having the initial value of zero, and as shown in the figure the same general behavior is observed. The 10 torr cavity pressure results for scale Λ are also plotted for comparison. For the 10 torr case the correlation rapidly drops to negligible values. For $p = 100$ torr, $\overline{\alpha'\beta'}/\bar{\alpha}\bar{\beta}$ has fairly substantial values for the entire flowfield and approaches -1 at large downstream distances. This behavior is consistent with the results presented earlier (Ref. 1) showing the variation of $\overline{\alpha'\beta'}/\bar{\alpha}\bar{\beta}$ with Damköhler number. The mixedness correlation in a free shear layer approaches -1 at large Damköhler numbers.

The effect of the initial turbulence amplitude on DF(2) formation is shown in Figures 24 and 25. Figure 24 shows the profiles of DF(2) at 2.5 cm distance downstream of the nozzle exit for laminar flow and $\overline{u'u'}_{init} = .004$ and $.04$. The profiles are somewhat different but the peak DF(2) mole fractions are nearly the same. The integrated DF(2) formation as a function of the axial position is presented in Figure 25, and indicates somewhat larger production of excited species for

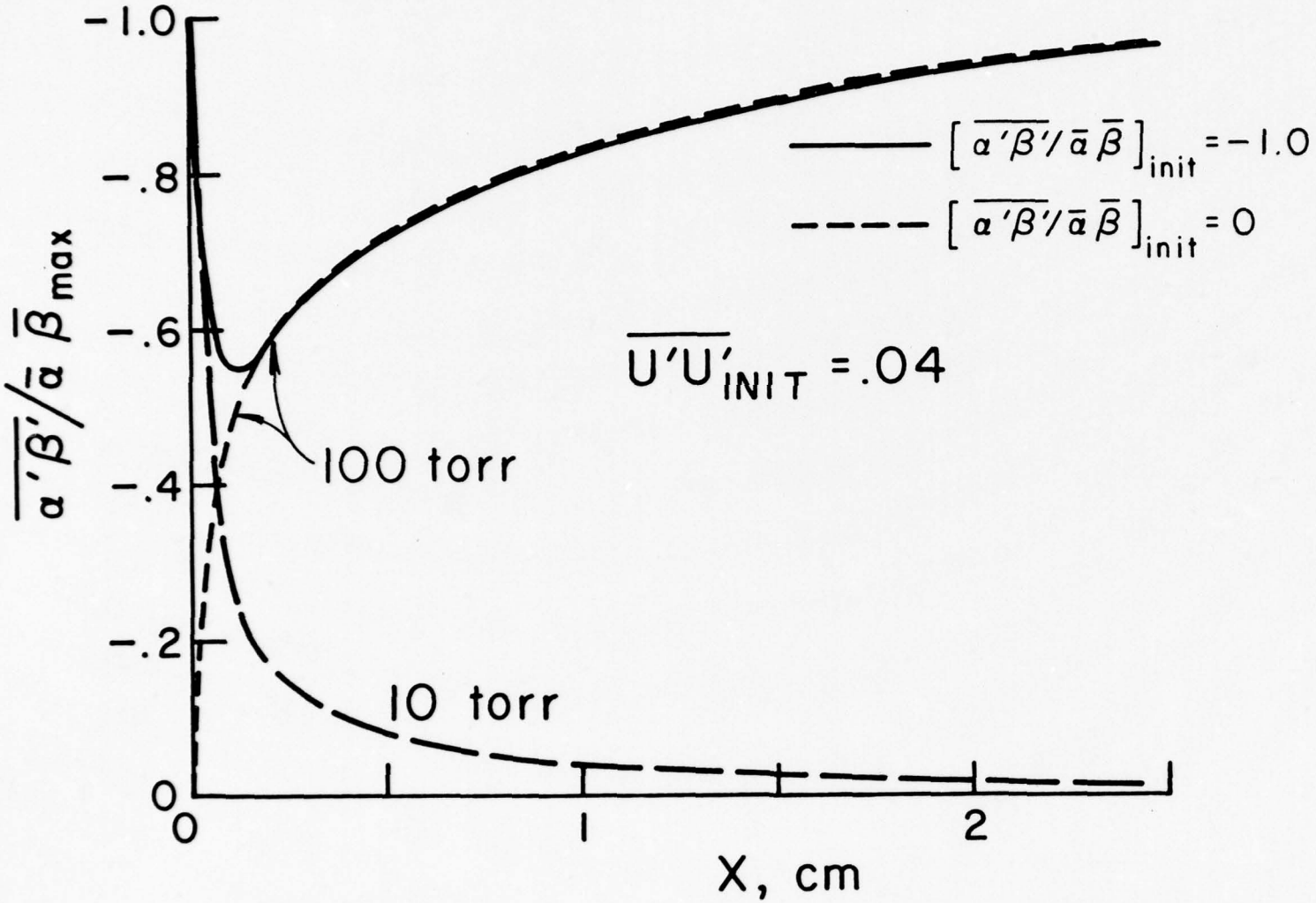

Figure 23. Behavior of the mixedness correlation at two different cavity pressures.

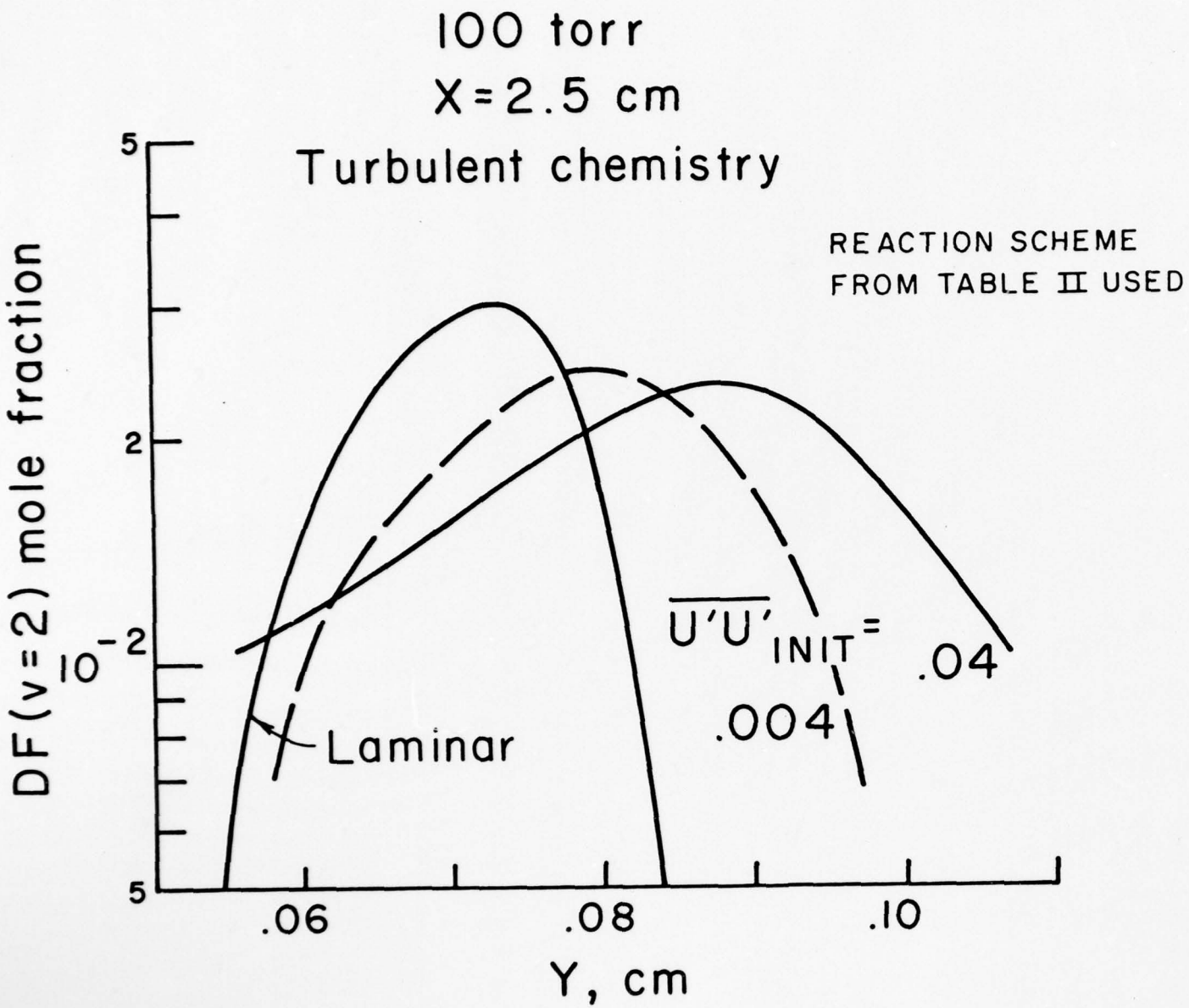

Figure 24. Effect of various initial turbulence levels on DF(2) formation.

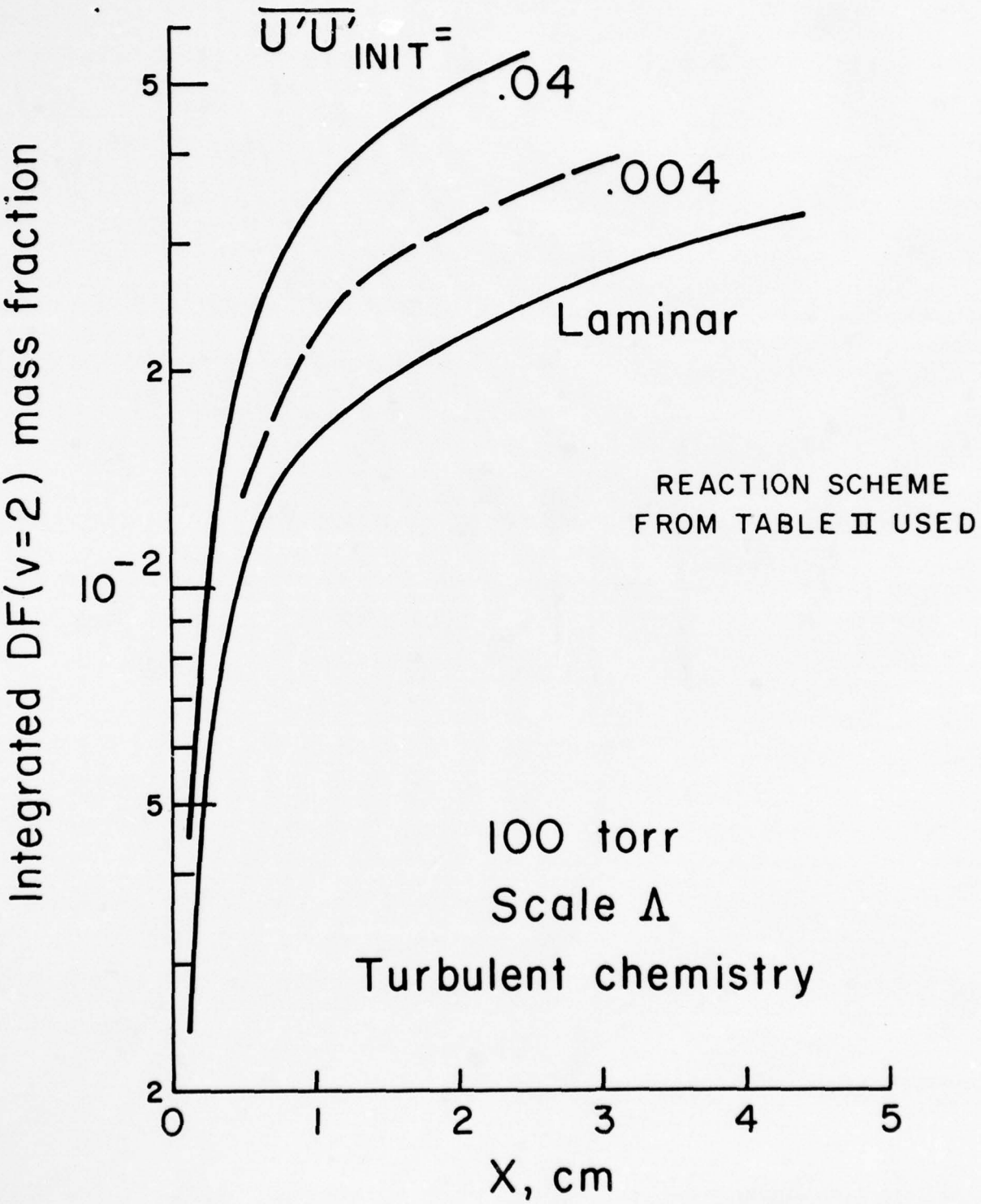

Figure 25. Effect of various initial turbulence levels on integrated DF(2) production.

larger initial disturbance amplitudes. The effect of scale variations was not investigated for the 100 torr cavity pressure.

The effect of initial turbulence isotropy was investigated for the 100 torr pressure laser in the same manner as for the 10 torr case, and similar results were obtained. There are small differences in the DF(2) predictions very close to the nozzle exit, but further downstream there are only negligible differences among the cases that were investigated.

Figure 26 compares the predictions for DF(2) formation at X = 2.5 cm for p = 10 torr and p = 100 torr . The computations have the same initial turbulence amplitude and use the full "turbulent chemistry" formulation. The results show that significantly larger amounts of DF(2) (and other excited vibration levels) are produced. However, as the complete set of deactivation processes is not included, we cannot predict whether or not this translates into improved laser performance.

Figure 27 shows the typical axial variation of DF(v) and the temperature in the central region of the flow for 100 torr cavity pressure. These results were calculated using the turbulent chemistry formulation, and the reaction scheme in Table 1. The results were somewhat surprising in the fact that the predictions showed DF(3) and DF(2) larger than DF(1). The runs were repeated with the more complete reaction scheme of Table 2 and virtually the same results were obtained. To further verify the basic correctness of the RSL program and the multi-step reaction procedure being used in the program, the calculations were also repeated using an eddy viscosity, laminar chemistry code available at A.R.A.P. (Low Altitude Plume Program or LAPP), and the same trends in the DF(v) axial profiles were predicted. Therefore, the Reacting Shear Layer program calculations with the use of the reaction schemes outlined in Tables 1 and 2 appear to be correct. Calculations should be performed with the use of a more complete reaction scheme in

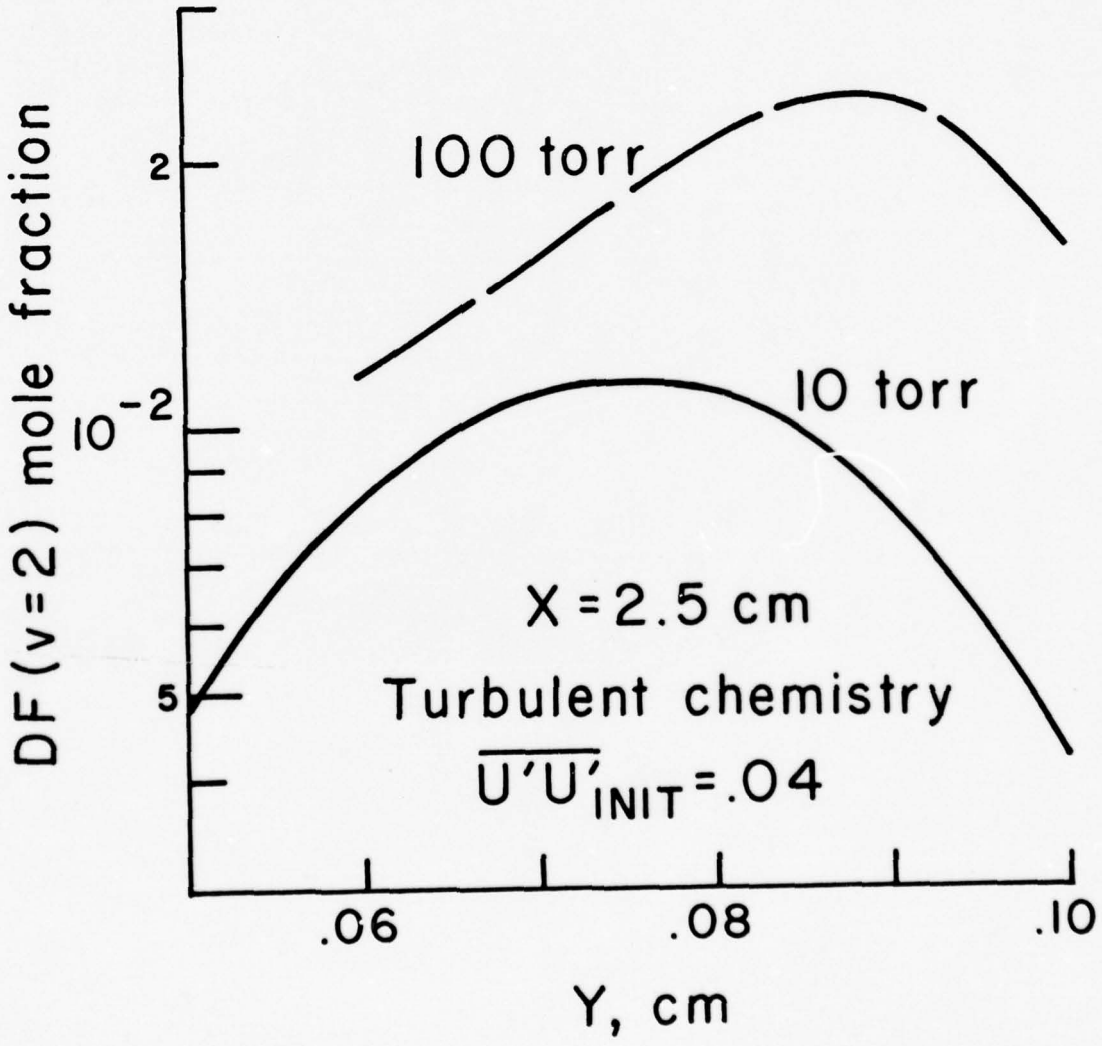

Figure 26. Effect of cavity pressure on DF(2) production.

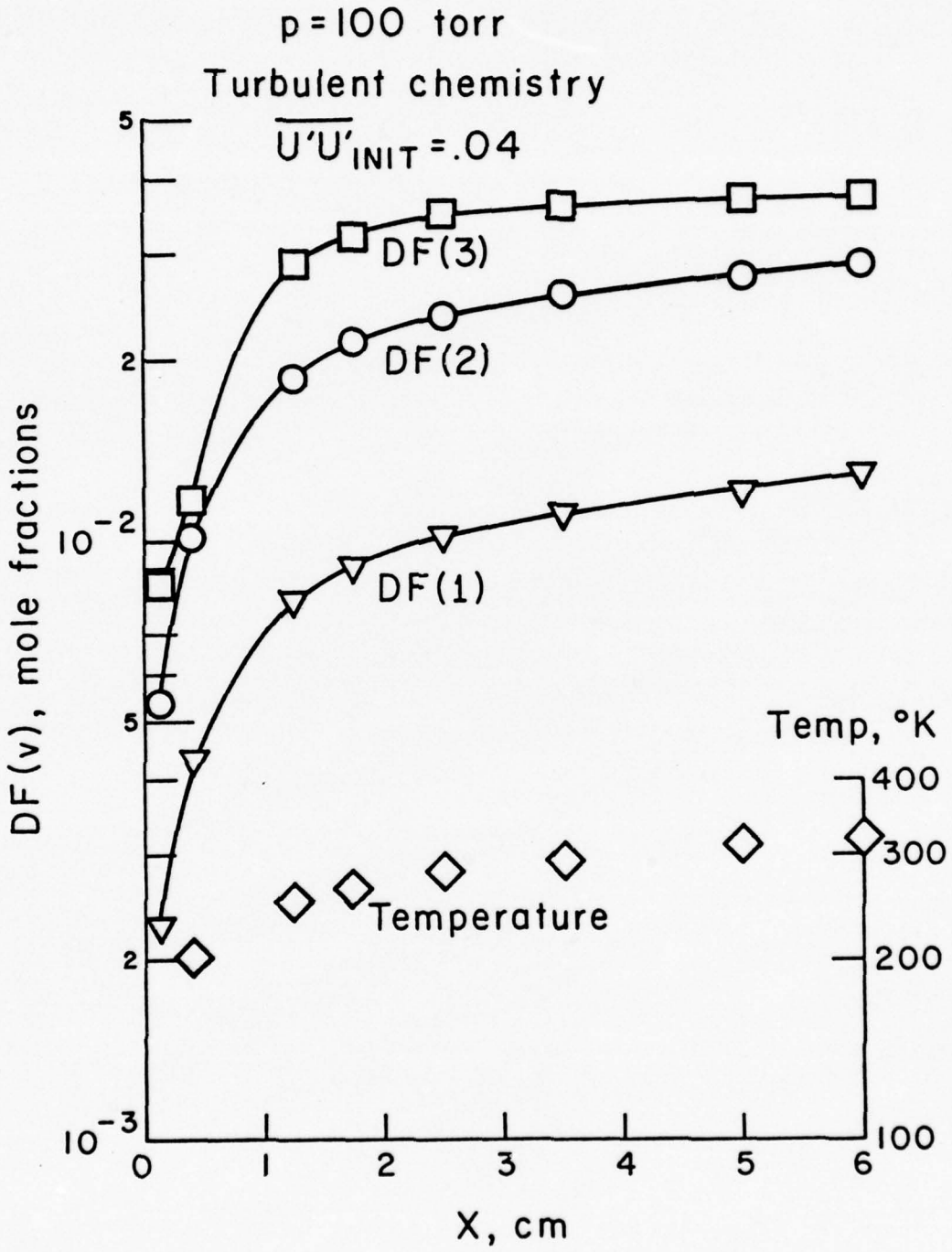

Figure 27. Typical axial profiles of DF(v) and temperature.

our program for detailed comparison with experimental measurements in chemical laser systems.

These calculations for DF chemical lasers using our complete second-order closure program have clearly demonstrated the significant effects of the turbulence characteristics on the performance of chemical lasers operating in the transitional flow regime. Significant turbulence-chemistry interactions could be present at somewhat higher flow Reynolds numbers. The above calculations have to be repeated with the "typical eddy" model to check the sensitivity of the results to the pdf models for the higher-order scalar correlations. Further, the more complete reaction set of laser kinetics should be used in the program to compare the program predictions to experimental measurements and to predict the effect of turbulence parameters on actual laser systems.

VI. SUMMARY AND CONCLUSIONS

A complete second-order closure program for the study of turbulent reacting shear flows has been developed. The program is capable of handling multi-species, multi-step chemical reactions and includes turbulence-chemistry interaction effects in the analysis.

The program has been used to study the mixing and chemical reactions in the initial region of a supersonic DF chemical laser. The effects of a number of turbulence variables — intensity q^2, scale Λ, and the mixedness correlation $\overline{\alpha'\beta'}/\bar{\alpha}\bar{\beta}$ — on the formation of vibrationally excited DF(v) species have been studied. The studies at low pressure (10 torr) demonstrate the need for a second-order approach to predict the details of the transitional turbulent flow. There are very significant effects of the initial turbulence amplitude and turbulence scale on the formation of DF(v). Different combinations of q^2 and Λ could lead to improvement or degradation in laser performance. At higher cavity pressures (100 torr), the flowfield has a significant level of turbulence and there are important turbulence-chemistry interaction effects that must be taken into account. Significant errors can result from the neglect of the mixedness correlations in the chemical source terms for finite rate chemistry calculations.

The important conclusions of the study for the MESA IV flow parameters are summarized in the table below:

Pressure	Effect on DF(v) Formation of:			
	q^2_{init}	Turbulence Isotropy	Λ	$\overline{\alpha'\beta'}/\bar{\alpha}\bar{\beta}$
10 torr	Strong	Weak	Strong	Weak
100 torr	Strong	Weak	-	Strong

These studies have clearly demonstrated some of the important effects in nonequilibrium turbulent flowfields that can only be analyzed using a second-order closure program. The A.R.A.P. Reacting Shear Layer (RSL) program has now reached the stage of development wherein it can be used for the analysis of complex turbulent reacting flowfields.

VII. NOMENCLATURE

a	turbulence model parameter
A	turbulence model parameter
b	slit width, also turbulence model parameter
g_{ij}	matrix tensor
h	sensible enthalpy
k	thermal conductivity reaction rate
ℓ_u	half width of velocity profile
ℓ_θ	half width of temperature profile
p	pressure
q^2	turbulence kinetic energy
s	turbulence model parameter
T	temperature
u_i or u, v, w	velocity components
V_c	turbulence model parameter
x, X	axial coordinate
y	normal coordinate
$y_{.75}$, $y_{.25}$	position in flow where $\bar{u} - \bar{u}_2/\bar{u}_1 - \bar{u}_2 = .75, .25$
α, β, γ	species mass fractions
θ	$T - T_{ambient}$
Λ	turbulent macroscale
λ	turbulent microscale
ρ	density

Superscripts

$\overline{\quad}$, $\langle\rangle$	denotes time average
$'$	denotes fluctuation about the mean value

VIII. REFERENCES

1. Varma, A.K., R.A. Beddini, and E.S. Fishburne, "Second-Order Closure Analysis of Turbulent Reacting Flows," Proceedings of the 1976 Heat Transfer and Fluid Mechanics Institute (A.A. McKillop, J.W. Baughn, H.A. Dwyer, eds.), Stanford University Press, 1976.

2. Fishburne, E.S., R.A. Beddini, and A.K. Varma, "The Computation of Afterburning Rocket Exhaust Plumes," A.R.A.P. Report No. 283, July 1976.

3. Launder, B.E. and D.B. Spalding, Mathematical Models of Turbulence, Academic Press, New York and London, 1972.

4. Bradshaw, P., "The Understanding and Prediction of Turbulent Flow," Aeronautical Journal, 16, 1972, pp. 403-418.

5. Saffman, P.G., "A Model for Inhomogeneous Turbulent Flow," Proceedings of Royal Society of London, 317, 1970, pp. 417-433.

6. Varma, A.K., R.A. Beddini, R.D. Sullivan, and C. duP. Donaldson, "Application of an Invariant Second-Order Closure Model to Compressible Turbulent Shear Layers," AIAA Paper No. 74-592, presented at the AIAA 7th Fluid and Plasma Dynamics Conference, Palo Alto, CA, June 17-19, 1974.

7. Lewellen, W.S., M.E. Teske, and C. duP. Donaldson, "Turbulence Model of Diurnal Variations in the Planetary Boundary Layer," Proceedings of the 1974 Heat Transfer and Fluid Mechanics Institute (L.R. Davis and R.E. Wilson, eds.), Stanford University Press, 1974, pp. 301-319.

8. Sullivan, R.D., "A Program to Compute the Behavior of a Three-Dimensional Turbulent Vortex," ARL-TR-74-0009, December 1973.

9. Finson, M.L., "Hypersonic Wake Aerodynamics at High Reynolds Numbers," AIAA Journal., 11, 8 August 1973, pp. 1137-1145.

10. Donaldson C. duP. and G.R. Hilst, "Chemical Reactions in Inhomogeneous Mixtures: The Effect of the Scale of Turbulent Mixing," Proceedings of the 1972 Heat Transfer and Fluid Mechanics Institute, Stanford University Press, Stanford, CA, pp. 256-261.

11. Spalding, D.B., "Mixing and Chemical Reaction in Steady Confined Turbulent Flames," 13th Symposium (International) on Combustion, The Combustion Institute, Pittsburgh, PA, 1971, pp. 645-657.

12. Spalding, D.B., "A General Theory of Turbulent Combustion, the LaGrangian Aspects," AIAA 77-141, presented at the AIAA 15th Aerospace Sciences Meeting, Los Angeles, CA, January 24-26, 1977.

13. Rhodes, R.P., P.T. Harsha, and C.E. Peters, "Turbulent Kinetic Energy Analyses of Hydrogen-Air Diffusion Flames," Acta Astronautica, 1, 1974, pp. 443-470.

14. Bray, K.N.C. and J.B. Moss, "A Unified Statistical Model of the Premixed Turbulent Flame," AASU Report No. 335, University of Southampton, November 1974.

15. Libby, P.A., "On Turbulent Flows with Fast Chemical Reactions. III. Two-Dimensional Mixing with Highly Dilute Reactants," Combustion Science and Technology (Special Issue on Turbulent Reactive Flows), Gordon and Breach Science Publishers, NY (in press).

16. Borghi, R. and P. Moreau, "Turbulent Combustion in a Premixed Flow," presented at the V Intl. Coll. on Gasdynamics of Explosions and Reactive Systems, Bourges, France, September 1975.

17. Kewley, D.J., "A Model of the Supersonic HF Chemical Mixing Laser Including Turbulence Effects on the Chemistry," presented at the D.G.L.R. Symposium on Gasdynamic and Chemical Lasers, Koln, W. Germany, October 1976.

18. Varma, A.K., "Second-Order Closure of Turbulent Reacting Shear Flows," A.R.A.P. Report No. 235, February 1975.

19. Donaldson, C. duP., "Atmospheric Turbulence and the Dispersal of Atmospheric Pollutants," EPA-R4-73-016a, Environmental Protection Agency, 1973.

20. Lewellen, W.S. and M.E. Teske, "Prediction of the Monin-Obukhov Similarity Functions from an Invariant Model of Turbulence," J. Atmospheric Sciences, Vol. 30, 1973, pp. 1340-1345.

21. Varma, A.K., R.A. Beddini, R.D. Sullivan, and E.S. Fishburne, "Turbulent Shear Flows in Laser Nozzles and Cavities," A.R.A.P. Report No. 231, October 1974.

22. Donaldson, C. duP., "On the Modeling of the Scalar Correlations Necessary to Construct a Second-Order Closure Description of Turbulent Reacting Flows," Turbulent Mixing in Nonreactive and Reactive Flows (S.N.B. Murthy, ed.), Plenum Press, New York, 1975, pp. 131-162.

23. Donaldson, C. duP. and A.K. Varma, "Remarks on the Construction of a Second-Order Closure Description of Turbulent Reacting Flows," Combustion Science and Technology (Special Issue on Turbulent Reactive Flows), Gordon and Breach Science Publishers, NY (in press).

24. Lewellen, W.S., "Use of Invariant Modeling," A R.A.P. Report No. 243, April 1975.

25. Chevray, R. and L.S.G. Kovasznay, "Turbulent Measurements in the Wake of a Thin Flat Plate," AIAA Journal, Vol. 7, No. 8, August 1969.

26. Kline, S.J., D.E. Coles, J.M. Eggers, and P.T. Harsha, "Experiments in Free Shear Flows - Status and Needs for the Future," Free Turbulent Shear Flows, Vol I, Conference Proceedings, Vol. II, Summary of Data, NASA SP 321, 1973.

27. Davis, A.E., J.F. Keffer, and W.D. Baines, "Spread of a Heated Plane Turbulent Jet," The Physics of Fluids, Vol 18, No. 7, July 1975.

28. Uberoi, M.S. and P.I. Singh, "Turbulent Mixing in a Two-Dimensional Jet," The Physics of Fluids, Vol. 18, No. 7, July 1975.

29. Konrad, J.H., "An Experimental Investigation of Mixing in Two-Dimensional Turbulent Shear Flows with Applications to Diffusion-Limited Chemical Reactions," Ph.D. Thesis, California Institute of Technology, Pasadena, CA, 1976.

30. Fishburne, E.S., A.K. Varma, and C. duP. Donaldson, "Aspects of Turbulent Combustion," AIAA 77-100, presented at the AIAA 15th Aerospace Sciences Meeting, Los Angeles, CA, January 24-26, 1977.

31. Cohen, N., "A Brief Review of Rate Coefficients for Reactions in the D_2-F_2 Chemical System," SAMSO-TR-74-14, January 1974.

TABLE 1. DF CHEMICAL LASER REACTION SET

$K_F = A*EXP(B/RT)/T**N$

	REACTIONS							(MOLES-ML-SEC UNITS)		
								A	N	B
1	F	+	D2	=	DF1	+	D	0.1929E 16	0.9	-2000.0
2	F	+	D2	=	DF2	+	D	0.4582E 16	0.9	-2000.0
3	F	+	D2	=	DF3	+	D	0.7235E 16	0.9	-2000.0
4	F	+	D2	=	DF4	+	D	0.5426E 16	0.9	-2000.0
5	DF1	+	DFO	=	DFO	+	DFO	0.1025E 03	-2.9	3200.0
6	DF2	+	DFO	=	DF1	+	DFO	0.1989E 03	-2.9	3200.0
7	DF3	+	DFO	=	DF2	+	DFO	0.3015E 03	-2.9	3200.0
8	DF4	+	DFO	=	DF3	+	DFO	0.4040E 03	-2.9	3200.0
9	DF1	+	D2	=	DFO	+	D2	0.5607E 02	-3.0	0.0
10	DF2	+	D2	=	DF1	+	D2	0.1145E 03	-3.0	0.0
11	DF3	+	D2	=	DF2	+	D2	0.1688E 03	-3.0	0.0
12	DF4	+	D2	=	DF3	+	D2	0.2231E 03	-3.0	0.0
13	DF1	+	F	=	DFO	+	F	0.2834E 16	0.7	-3600.0
14	DF2	+	F	=	DF1	+	F	0.3316E 16	0.7	-3600.0
15	DF3	+	F	=	DF2	+	F	0.4462E 16	0.7	-3600.0
16	DF4	+	F	=	DF3	+	F	0.8441E 16	0.7	-3600.0

TABLE 2. DF CHEMICAL LASER REACTION SET

$K_F = A*EXP(B/RT)/T**N$

	REACTIONS							(MOLES-ML-SEC UNITS)		
								A	N	B
1	F	+	D2	=	DF1	+	D	0.1929E 16	0.9	-2000.0
2	F	+	D2	=	DF2	+	D	0.4582E 16	0.9	-2000.0
3	F	+	D2	=	DF3	+	D	0.7235E 16	0.9	-2000.0
4	F	+	D2	=	DF4	+	D	0.5426E 16	0.9	-2000.0
5	DF1	+	M	=	DF0	+	M	0.1025E 03	-2.9	3200.0
6	DF2	+	M	=	DF1	+	M	0.2050E 03	-2.9	3200.0
7	DF3	+	M	=	DF2	+	M	0.3075E 03	-2.9	3200.0
8	DF4	+	M	=	DF3	+	M	0.4100E 03	-2.9	3200.0
	WHERE $M = \sum_{0-4} DF(v)$									
9	DF1	+	D2	=	DF0	+	D2	0.5607E 02	-3.0	0.0
10	DF2	+	D2	=	DF1	+	D2	0.1145E 03	-3.0	0.0
11	DF3	+	D2	=	DF2	+	D2	0.1688E 03	-3.0	0.0
12	DF4	+	D2	=	DF3	+	D2	0.2231E 03	-3.0	0.0
13	DF1	+	F	=	DF0	+	F	0.2834E 16	0.7	-3600.0
14	DF2	+	F	=	DF1	+	F	0.3316E 16	0.7	-3600.0
15	DF3	+	F	=	DF2	+	F	0.4462E 16	0.7	-3600.0
16	DF4	+	F	=	DF3	+	F	0.8441E 16	0.7	-3600.0
17	DF1	+	HE	=	DF0	+	HE	0.1561E-05	-5.0	0.0
18	DF2	+	HE	=	DF1	+	HE	0.3123E-05	-5.0	0.0
19	DF3	+	HE	=	DF2	+	HE	0.4685E-05	-5.0	0.0
20	DF4	+	HE	=	DF3	+	HE	0.6271E-05	-5.0	0.0

APPENDIX A. GENERAL CONSERVATION EQUATIONS FOR A TURBULENT MULTICOMPONENT REACTING SYSTEM

Continuity Equation

$$\rho_t + (\rho u^\ell)_{,\ell} = 0 \tag{1}$$

Momentum Equation

$$\rho u_{j_t} + \rho u^\ell u_{j,\ell} = -p_{,j} + \tau^\ell_{j,\ell} \tag{2}$$

where

$$\tau^\ell_j = g^{\ell k}\mu\left(u_{j,k} + u_{k,j}\right) + \delta^\ell_j \mu^* u^k_{,k} \tag{3}$$

Energy Equation

$$\rho h_t + \rho u^\ell h_{,\ell} - p_t - u^\ell p_{,\ell} = \psi - \sum_\alpha h^o_\alpha \dot{w}_\alpha \tag{4}$$

where

$$h = \sum_\alpha h_\alpha \cdot c_\alpha \tag{5}$$

$$h_\alpha = \int_{T^o}^{T} c_{p_\alpha}\, dT \tag{6}$$

$$\psi = \phi - H \tag{7}$$

$$\phi = \tau^m_\ell u^\ell_{,m} \tag{8}$$

$$H = -g^{\ell m}\left[kT_{,\ell} + \rho \sum h_\alpha D_\alpha c_{\alpha,\ell}\right]_{,m} \tag{9}$$

Species Equation

$$\begin{aligned} \rho c_{\alpha_t} + \rho u^\ell c_{\alpha,\ell} &= \dot{w}_\alpha + g^{\ell m}\left(\rho D_\alpha c_{\alpha,\ell}\right)_{,m} \\ &= \dot{w}_\alpha + G_\alpha \end{aligned} \tag{10}$$

Equation of State

$$p = \rho \mathcal{R} T \sum \frac{c_\alpha}{W_\alpha} \tag{11}$$

In the above-noted equations, the symbols have their usual meaning: $\dot{w}_\alpha$ is the mass rate of formation of component α per unit volume; h^o_α is the heat of formation of species α ; D_α is the diffusion coefficient; and W_α is the species molecular weight.

Writing the dependent variables in these equations as the sum of a mean and a fluctuating part ($u = \bar{u} + u'$; $\rho = \bar{\rho} + \rho'$; etc.), one can derive equations for the mean quantities and the second-order correlations of the fluctuations.

Defining $\bar{\mathcal{D}} f = f_t + \bar{u}^\ell f_{,\ell}$, the equations can be written as

$$\bar{\mathcal{D}}\bar{\rho} + \bar{\rho}\bar{u}^\ell_{,\ell} + (\overline{\rho' u'^\ell})_{,\ell} = 0 \tag{12}$$

$$\bar{\rho}\bar{\mathcal{D}}\bar{u}_j + \overline{\rho' u'^\ell}\,\bar{u}_{j,\ell} + (\overline{\rho' u'_j})_t + \left[\bar{\rho}(\overline{u'^\ell u'_j}) + \bar{u}^\ell(\overline{\rho' u'_j}) + (\overline{\rho' u'^\ell u'_j})\right]_{,\ell} = -\bar{p}_{,j} + \bar{\tau}^\ell_{j,\ell} \tag{13}$$

$$\bar{\rho}\bar{\mathcal{D}}\bar{h} + \overline{\rho' u'^\ell}\,\bar{h}_{,\ell} + (\overline{\rho' h'})_t + \left[\bar{\rho}(\overline{u'^\ell h'}) + \bar{u}^\ell(\overline{\rho' h'}) + (\overline{\rho' u'^\ell h'})\right]_{,\ell} = \bar{p}_t + \bar{u}^\ell \bar{p}_{,\ell} + (\overline{u'^\ell p'_{,\ell}}) + \bar{\psi} - \sum_\alpha h^o_\alpha \bar{\dot{w}}_\alpha \tag{14}$$

$$\bar{\rho}\bar{\mathcal{D}}\bar{c}_\alpha + (\overline{\rho' u'^\ell})\bar{c}_{\alpha,\ell} + (\overline{\rho' c'_\alpha})_t + \left[\bar{\rho}(\overline{u'^\ell c'_\alpha}) + \bar{u}^\ell(\overline{\rho' c'_\alpha}) + (\overline{\rho' u'^\ell c'_\alpha})\right]_{,\ell} = \bar{\dot{w}}_\alpha + \bar{G}_\alpha \tag{15}$$

$$\bar{\rho}\,\bar{\mathcal{D}}(\overline{u_j'u_k'}) + (\overline{\rho' u_j' u_k'})_t + \left[\bar{\rho}(\overline{u'^{\ell} u_j' u_k'}) + \bar{u}^{\ell}(\overline{\rho' u_j' u_k'}) + (\overline{\rho' u'^{\ell} u_j' u_k'})\right]_{,\ell}$$

$$- (\overline{\rho' u'^{\ell}})_{,\ell}(\overline{u_j' u_k'}) + (\overline{\rho' u_k'})\bar{\mathcal{D}}\,\bar{u}_j + (\overline{\rho' u_j'})\bar{\mathcal{D}}\,\bar{u}_k$$

$$+ (\overline{u'^{\ell} u_k'})\bar{\rho}\bar{u}_{j,\ell} + (\overline{u'^{\ell} u_j'})\bar{\rho}\bar{u}_{k,\ell} + (\overline{\rho' u'^{\ell} u_k'})\bar{u}_{j,\ell}$$

$$+ (\overline{\rho' u'^{\ell} u_j'})\bar{u}_{k,\ell}$$

$$= -(\overline{u_k' p'_{,j}}) + (\overline{u_j' p'_{,k}}) + (\overline{u_k' \tau'^{\ell}_{j,\ell}}) + (\overline{u_j' \tau'^{\ell}_{k,\ell}}) \qquad (16)$$

$$\bar{\rho}\,\bar{\mathcal{D}}(\overline{h'h'}) + (\overline{\rho h' h'})_t + \left[\bar{\rho}(\overline{u'^{\ell} h' h'}) + \bar{u}^{\ell}(\overline{\rho' h' h'}) + (\overline{\rho' u'^{\ell} h' h'})\right]_{,\ell}$$

$$- (\overline{\rho' u'^{\ell}})_{,\ell}(\overline{h' h'}) + 2(\overline{\rho' h'})\bar{\mathcal{D}}\,\bar{h} + 2\bar{\rho}\bar{h}_{,\ell}(\overline{u'^{\ell} h'})$$

$$+ 2\bar{h}_{,\ell}(\overline{\rho' u'^{\ell} h'})$$

$$= 2(\overline{h' p_t'}) + 2\bar{u}^{\ell}(\overline{h' p'_{,\ell}}) + 2\bar{p}_{,\ell}(\overline{h' u'^{\ell}}) + 2(\overline{h' u'^{\ell} p'_{,\ell}})$$

$$+ 2(\overline{h'\psi'}) - 2\sum_{\alpha} h_{\alpha}^{o}\,(\overline{h' \dot{w}_{\alpha}'}) \qquad (17)$$

$$\bar{\rho}\bar{\mathcal{D}}(\overline{u_j'h'}) + (\overline{\rho'u_j'h'})_t + \left[\bar{\rho}(\overline{u'^{\ell}u_j'h'}) + \bar{u}^{\ell}(\overline{\rho'u_j'h'}) + (\overline{\rho'u'^{\ell}u_j'h'})\right]_{,\ell}$$

$$- (\overline{\rho'u'^{\ell}})_{,\ell}(\overline{u_j'h'}) + (\overline{\rho'u_j'})\bar{\mathcal{D}}\bar{h} + (\overline{\rho'h'})\bar{\mathcal{D}}\bar{u}_j$$

$$+ (\overline{u'^{\ell}u_j'})\bar{\rho}\bar{h}_{,\ell} + (\overline{u'^{\ell}h'})\bar{\rho}\bar{u}_{j,\ell} + (\overline{\rho'u'^{\ell}u_j'})\bar{h}_{,\ell}$$

$$+ (\overline{\rho'u'^{\ell}h'})\bar{u}_{j,\ell}$$

$$= (\overline{u_j'p_t'}) + \bar{u}^{\ell}(\overline{u_j'p'_{,\ell}}) + \bar{p}_{,\ell}(\overline{u_j'u'^{\ell}}) + (\overline{u_j'u'^{\ell}p'_{,\ell}}) + (\overline{u_j'\psi'})$$

$$- \sum_{\alpha} h_{\alpha}^{o}(\overline{u_j'\dot{w}_{\alpha}'}) - (\overline{h'p'_{,j}}) + (\overline{h'\tau'^{\ell}_{j,\ell}}) \qquad (18)$$

$$\bar{\mathcal{D}}(\overline{\rho'\rho'}) + 2\bar{\rho}_{,\ell}(\overline{\rho'u'^{\ell}}) + 2\bar{u}^{\ell}_{,\ell}(\overline{\rho'\rho'}) + 2\bar{\rho}(\overline{\rho'u'^{\ell}_{,\ell}})$$

$$+ (\overline{\rho'\rho'u'^{\ell}_{,\ell}}) + (\overline{\rho'\rho'u'^{\ell}})_{,\ell} = 0 \qquad (19)$$

$$\bar{\rho}\bar{\mathcal{D}}(\overline{c_{\alpha}'c_{\beta}'}) + (\overline{\rho'c_{\alpha}'c_{\beta}'})_t + \left[\bar{\rho}(\overline{u'^{\ell}c_{\alpha}'c_{\beta}'}) + \bar{u}^{\ell}(\overline{\rho'c_{\alpha}'c_{\beta}'}) + (\overline{\rho'u'^{\ell}c_{\alpha}'c_{\beta}'})\right]_{,\ell}$$

$$- (\overline{\rho'u'^{\ell}})_{,\ell}(\overline{c_{\alpha}'c_{\beta}'}) + (\overline{\rho'c_{\beta}'})\bar{\mathcal{D}}\bar{c}_{\alpha} + (\overline{\rho'c_{\alpha}'})\bar{\mathcal{D}}\bar{c}_{\beta}$$

$$+ (\overline{u'^{\ell}c_{\beta}'})\bar{\rho}\bar{c}_{\alpha,\ell} + (\overline{u'^{\ell}c_{\alpha}'})\bar{\rho}\bar{c}_{\beta,\ell} + (\overline{\rho'u'^{\ell}c_{\beta}'})\bar{c}_{\alpha,\ell}$$

$$+ (\overline{\rho'u'^{\ell}c_{\alpha}'})\bar{c}_{\beta,\ell}$$

$$= (\overline{c_{\beta}'\dot{w}_{\alpha}'}) + \overline{c_{\alpha}'\dot{w}_{\beta}'} + (\overline{c_{\beta}'G_{\alpha}'}) + \overline{c_{\alpha}'G_{\beta}'} \qquad (20)$$

$$\bar{\rho}\mathcal{D}(\overline{u_j'c_\alpha'}) + (\overline{\rho'u_j'c_\alpha'})_t + \left[\bar{\rho}(\overline{u'^{\ell}u_j'c_\alpha'}) + \bar{u}^{\ell}(\overline{\rho'u_j'c_\alpha'}) + (\overline{\rho'u'^{\ell}u_j'c_\alpha'})\right]_{,\ell}$$

$$- (\overline{\rho'u'^{\ell}})_{,\ell}(\overline{u_j'c_\alpha'}) + (\overline{\rho'u_j'})\mathcal{D}\bar{c}_\alpha + (\overline{\rho'c_\alpha'})\mathcal{D}\bar{u}_j$$

$$+ (\overline{u'^{\ell}u_j'})\bar{\rho}\bar{c}_{\alpha,\ell} + (\overline{u'^{\ell}c_\alpha'})\bar{\rho}\bar{u}_{j,\ell} + (\overline{\rho'u'^{\ell}u_j'})\bar{c}_{\alpha,\ell}$$

$$+ (\overline{\rho'u'^{\ell}c_\alpha'})\bar{u}_{j,\ell}$$

$$= (\overline{u_j'\dot{w}_\alpha'}) + (\overline{u_j'G_\alpha'}) - (\overline{c_\alpha'p'_{,j}}) + (\overline{c_\alpha'\tau_{j,\ell}'^{\ell}}) \qquad (21)$$

$$\bar{\rho}\mathcal{D}(\overline{h'c_\alpha'}) + (\overline{\rho'h'c_\alpha'})_t + \left[\bar{\rho}(\overline{u'^{\ell}h'c_\alpha'}) + \bar{u}^{\ell}(\overline{\rho'h'c_\alpha'}) + (\overline{\rho'u'^{\ell}h'c_\alpha'})\right]_{,\ell}$$

$$- (\overline{\rho'u'^{\ell}})_{,\ell}(\overline{h'c_\alpha'}) + (\overline{\rho'h'})\mathcal{D}\bar{c}_\alpha + (\overline{\rho'c_\alpha'})\mathcal{D}\bar{h}$$

$$+ (\overline{u'^{\ell}h'})\bar{\rho}\bar{c}_{\alpha,\ell} + (\overline{u'^{\ell}c_\alpha'})\bar{\rho}\bar{h}_{,\ell} + (\overline{\rho'u'^{\ell}h'})\bar{c}_{\alpha,\ell}$$

$$+ (\overline{\rho'u'^{\ell}c_\alpha'})\bar{h}_{,\ell}$$

$$= (\overline{h'\dot{w}_\alpha'}) + (\overline{h'G_\alpha'}) + (\overline{c_\alpha'p_t'}) + \bar{u}^{\ell}(\overline{c_\alpha'p'_{,\ell}}) + \bar{p}_{,\ell}(\overline{c_\alpha'u'^{\ell}})$$

$$+ (\overline{c_\alpha'u'^{\ell}p'_{,\ell}}) + (\overline{c_\alpha'\psi'}) - \sum_\beta h_\beta^\circ(\overline{\dot{w}_\beta'c_\alpha'}) \qquad (22)$$

$$\bar{\rho}\bar{\mathcal{D}}(\overline{\rho' u_j'}) + (\overline{\rho'\rho' u_j'})_t + \left[\bar{\rho}(\overline{u'^{\ell}\rho' u_j'}) + \bar{u}^{\ell}(\overline{\rho'\rho' u_j'}) + (\overline{\rho'\rho' u'^{\ell} u_j'})\right]_{,\ell}$$

$$- (\overline{\rho' u'^{\ell}})_{,\ell}(\overline{\rho' u_j'}) + (\overline{\rho'\rho'})\bar{\mathcal{D}}\bar{u}_j + (\overline{\rho' u_j'})\bar{\mathcal{D}}\bar{\rho}$$

$$+ (\overline{u'^{\ell}\rho'})\bar{\rho}\bar{u}_{j,\ell} + (\overline{u'^{\ell} u_j'})\bar{\rho}\bar{\rho}_{,\ell} + (\overline{\rho'\rho' u'^{\ell}})\bar{u}_{j,\ell}$$

$$+ (\overline{\rho' u_j' u'^{\ell}})\bar{\rho}_{,\ell}$$

$$= -(\overline{\rho' p'_{,j}}) + (\overline{\rho' \tau_{j,\ell}'^{\ell}}) - \left[\bar{\rho}\bar{\rho}(\overline{u'^{\ell}_{,\ell} u_j'}) + 2\bar{\rho}\bar{u}^{\ell}_{,\ell}(\overline{\rho' u_j'})\right.$$

$$\left. + 2\bar{\rho}(\overline{\rho' u'^{\ell}_{,\ell} u_j'}) + \bar{u}^{\ell}_{,\ell}(\overline{\rho'\rho' u_j'}) + (\overline{\rho'\rho' u'^{\ell}_{,\ell} u_j'})\right] \tag{23}$$

$$\bar{\rho}\bar{\mathcal{D}}(\overline{\rho' h'}) + (\overline{\rho'\rho' h'})_t + \left[\bar{\rho}(\overline{u'^{\ell}\rho' h'}) + \bar{u}^{\ell}(\overline{\rho'\rho' h'}) + (\overline{\rho'\rho' u'^{\ell} h'})\right]_{,\ell}$$

$$- (\overline{\rho' u'^{\ell}})_{,\ell}(\overline{\rho' h'}) + (\overline{\rho'\rho'})\bar{\mathcal{D}}\bar{h} + (\overline{\rho' h'})\bar{\mathcal{D}}\bar{\rho}$$

$$+ (\overline{u'^{\ell}\rho'})\bar{\rho}\bar{h}_{,\ell} + (\overline{u'^{\ell} h'})\bar{\rho}\bar{\rho}_{,\ell} + (\overline{\rho'\rho' u'^{\ell}})\bar{h}_{,\ell} + (\overline{\rho' h' u'^{\ell}})\bar{\rho}_{,\ell}$$

$$= + (\overline{\rho' p_t'}) + \bar{u}^{\ell}(\overline{\rho' p'_{,\ell}}) + \bar{p}_{,\ell}(\overline{\rho' u'^{\ell}}) + (\overline{\rho' u'^{\ell} p'_{,\ell}})$$

$$+ (\overline{\rho'\psi'}) - \sum_{\alpha} h_{\alpha}^{o}(\overline{\rho' \dot{w}_{\alpha}'}) - \left[\bar{\rho}\bar{\rho}(\overline{u'^{\ell}_{,\ell} h'}) + 2\bar{\rho}\bar{u}^{\ell}_{,\ell}(\overline{\rho' h'})\right.$$

$$\left. + 2\bar{\rho}(\overline{\rho' h' u'^{\ell}_{,\ell}}) + \bar{u}^{\ell}_{,\ell}(\overline{\rho'\rho' h'}) + (\overline{\rho'\rho' h' u'^{\ell}_{,\ell}})\right] \tag{24}$$

$$\bar{\rho}\bar{\mathcal{D}}(\overline{\rho' c'_\alpha}) + (\overline{\rho'\rho' c'_\alpha})_t + \left[\bar{\rho}(\overline{u'^{\ell}\rho' c'_\alpha}) + \bar{u}^{\ell}(\overline{\rho'\rho' c'_\alpha}) + (\overline{\rho'\rho' u'^{\ell} c'_\alpha})\right]_{,\ell}$$

$$- (\overline{\rho' u'^{\ell}})_{,\ell}(\overline{\rho' c'_\alpha}) + (\overline{\rho'\rho'})\bar{\mathcal{D}}\bar{c}_\alpha + (\overline{\rho' c'_\alpha})\bar{\mathcal{D}}\bar{\rho}$$

$$+ (\overline{u'^{\ell}\rho'})\bar{\rho}\bar{c}_{\alpha,\ell} + (\overline{u'^{\ell} c'_\alpha})\bar{\rho}\bar{\rho}_{,\ell} + (\overline{\rho'\rho' u'^{\ell}})\bar{c}_{\alpha,\ell} + (\overline{\rho' c'_\alpha u'^{\ell}})\bar{\rho}_{,\ell}$$

$$= +(\overline{\rho' \dot{w}'_\alpha}) + (\overline{\rho' G'_\alpha}) - \left[\bar{\rho}\bar{\rho}(\overline{u'^{\ell}_{,\ell} c'_\alpha}) + 2\bar{\rho}\bar{u}^{\ell}_{,\ell}(\overline{\rho' c'_\alpha})\right.$$

$$\left. + 2\bar{\rho}(\overline{\rho' c'_\alpha u'^{\ell}_{,\ell}}) + \bar{u}^{\ell}_{,\ell}(\overline{\rho'\rho' c'_\alpha}) + (\overline{\rho'\rho' c'_\alpha u'^{\ell}_{,\ell}})\right] \tag{25}$$

Detailed expressions for terms like $\bar{\psi}$, ψ' , $\bar{G}_\alpha$, G'_α , etc. can be obtained from their definitions. The expressions for the reaction source terms $\bar{\dot{w}}_\alpha$ and $\dot{w}'_\alpha$ will be obtained from the modeling of the chemical reaction. As an example, if one uses a one-step chemical reaction model

$$\sum_{\alpha=1}^{N} \nu'_\alpha M_\alpha \rightarrow \sum_{\alpha=1}^{N} \nu''_\alpha M_\alpha \tag{26}$$

the reaction rate term can be written as

$$\dot{w}_\alpha = W_\alpha(\nu''_\alpha - \nu'_\alpha)\, A T^n \exp\left(-\frac{E}{\mathcal{R}T}\right) \prod_{\alpha=1}^{N} \left(\frac{\rho c_\alpha}{W_\alpha}\right)^{\nu'_\alpha} \tag{27}$$

Expressions for $\bar{\dot{w}}_\alpha$ and $\dot{w}'_\alpha$ can be obtained.